Overview of Swarm Mission

Octav Marghitu

Institute for Space Sciences, Bucharest, Romania

Workshop Bâlea-Paltinu

September 14–19, 2015

Photo: Jan Curtis, http://climate.gi.alaska.edu/Curtis

Swarm in a (biased) Nutshell

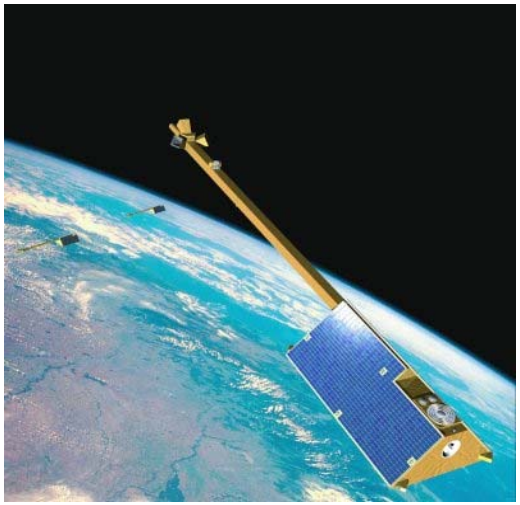

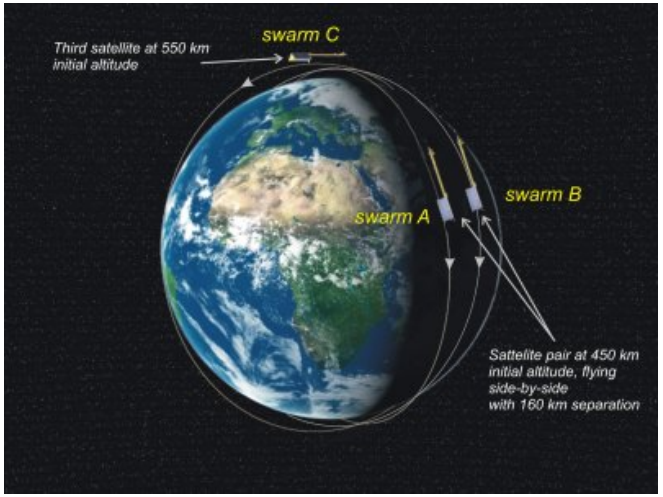

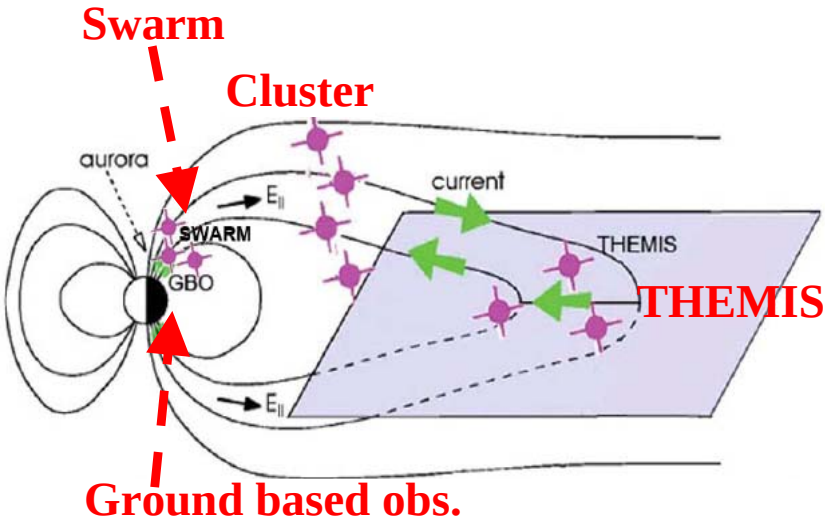

- ESA Earth Observation mission, launched on November 22, 2013
  - DLR CHAMP heritage.
  - Magnetic field from internal and external sources.
  - Magnetosphere–ionosphere coupling and aurora.
  - 3 satellites, 2 at ~450 km and one at ~550 km altitude.
  - Magnetic field, electric field, accelerometer, GPS receivers.
- All instruments are operational, except for Swarm-C/ASM (stopped on Nov. 5, 2014)
  - Magnetic field data (VFM, ASM) are available for scientific exploitation.
  - Provisional plasma data (TII, LP) released in Feb. 2015, though more CalVal work needed.
  - Accelerometer (ACC) data need further improvement and were not released yet.

Outline

- Mission overview
  - Science objectives
  - Experiments, Cal/Val activities, Data products
- Highlights (GRL Special Section)
  - Swarm Initial Field Model, mantle conductivity, crust magnetic field
  - EEF, ULF Pc3, Temperature anisotropy, Swarm/Cluster conjunction
- Activities at ISS
  - Field-aligned currents
  - Auroral electrodynamics

Science Objectives

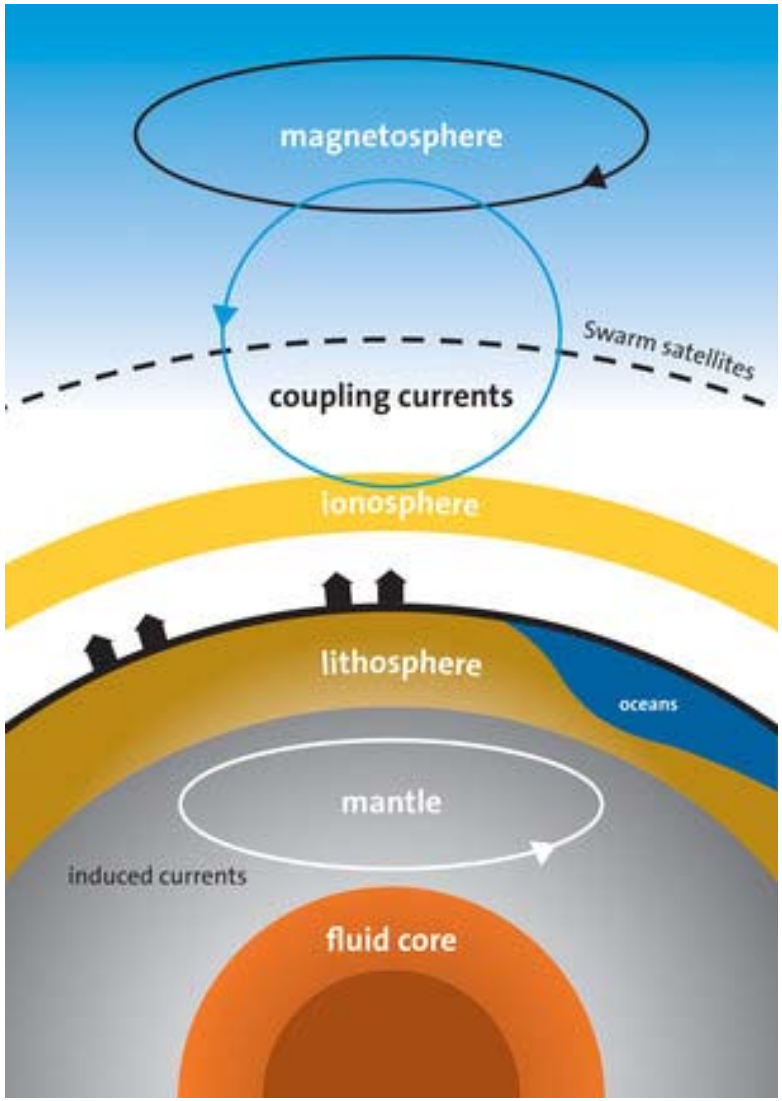

Credit: ESA

- Internal fields (VFM, ASM)
  - Studies of core dynamics, geodynamo processes, and core-mantle interaction
  - Mapping of the lithospheric magnetisation and its geological interpretation
  - Determination of the 3D electrical conductivity of the mantle
  - Identification of ocean circulation patterns by its magnetic signature
- External fields
  - Investigation of electric currents flowing in the magnetosphere and ionosphere (VFM. EFI)
  - Quantification of the magnetic forcing of the upper atmosphere, including studies of thermosphere densities and winds (ACC, GPS)

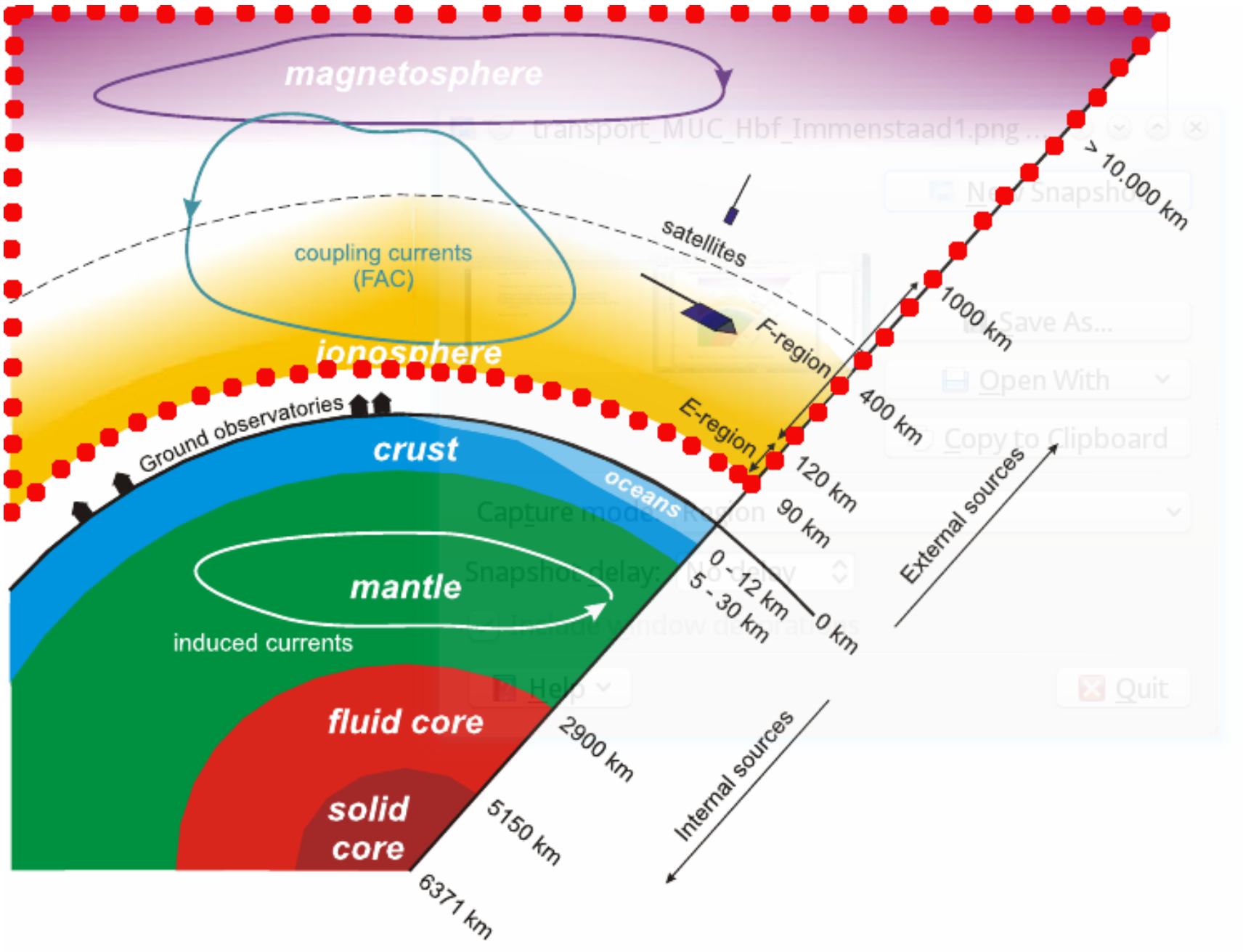

Sketch of the various sources contributing to the magnetic field measured by a LEO satellite (from Olsen et. al. Space Science Review 155, 65-93, 2010)

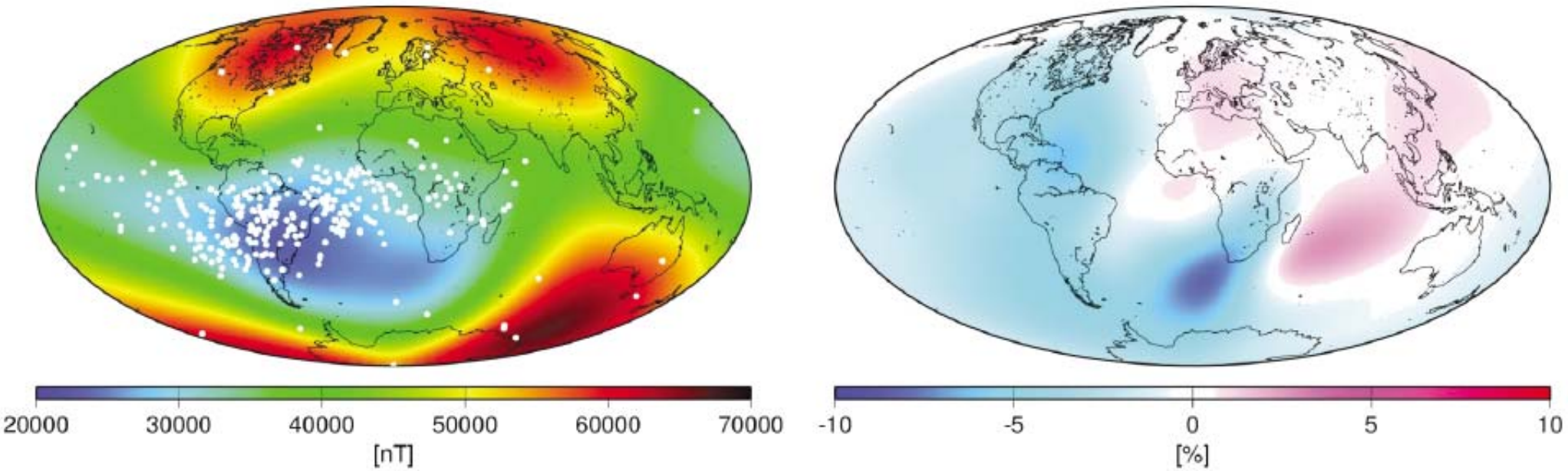

The geomagnetic field intensity at the Earth's surface with the South Atlantic Anomaly defined by the low values of the field. The white dots indicate positions where the TOPEX/Poseidon satellite experienced single event upsets (left). The change in field intensity over 20 years (from MAGSAT to Ørsted) is shown in percentage (right). From E. Friis-Christensen, H. Lühr, and G. Hulot, Earth Planets Space, 58, 351–358, 2006.

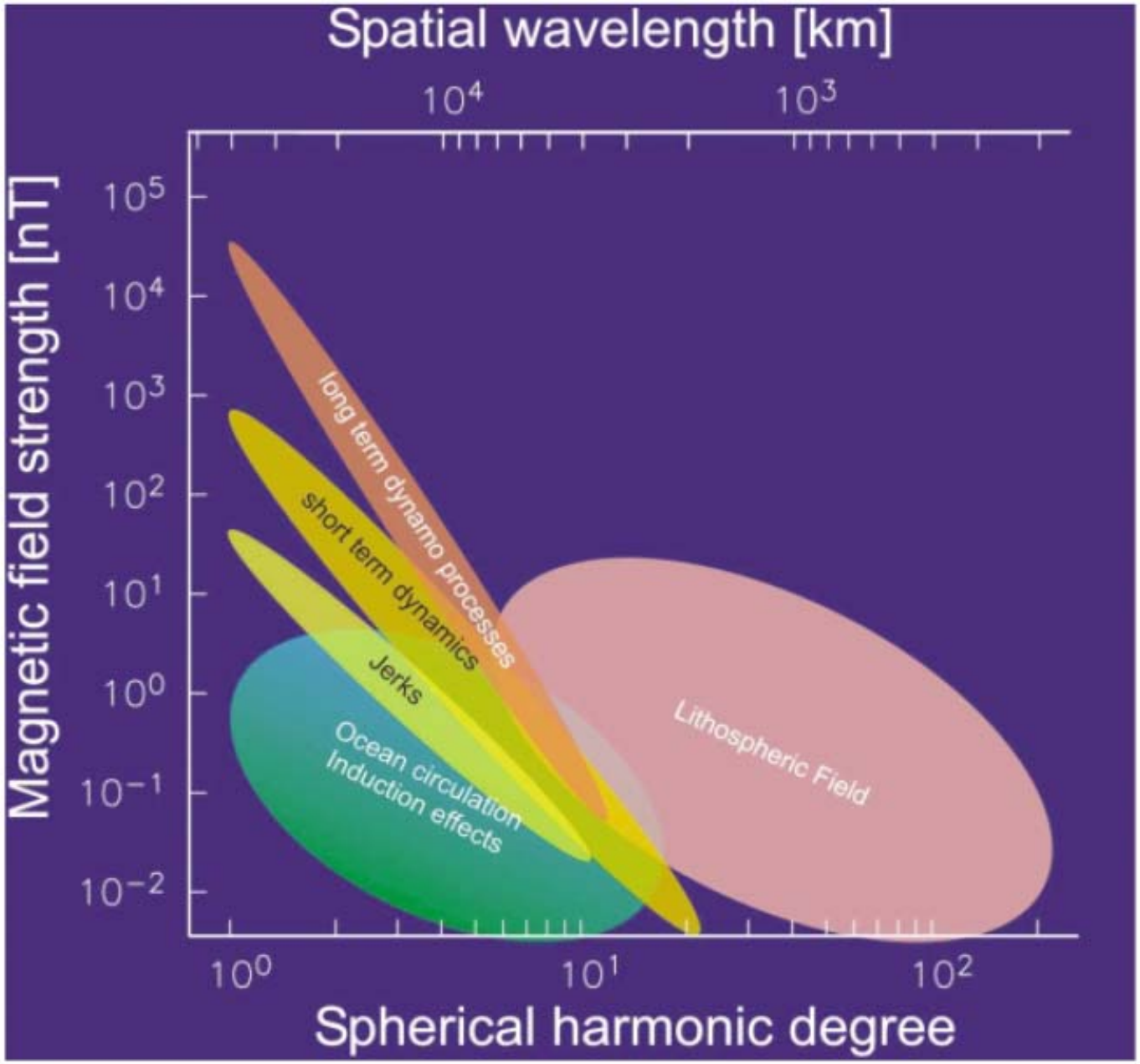

Signal amplitude at orbit altitude of the contributions from processes contributing to the magnetic field as a function of spatial scale. Source terms from within the solid Earth and the oceans. From E. Friis-Christensen, H. Lühr, and G. Hulot, Earth Planets Space, 58, 351–358, 2006.

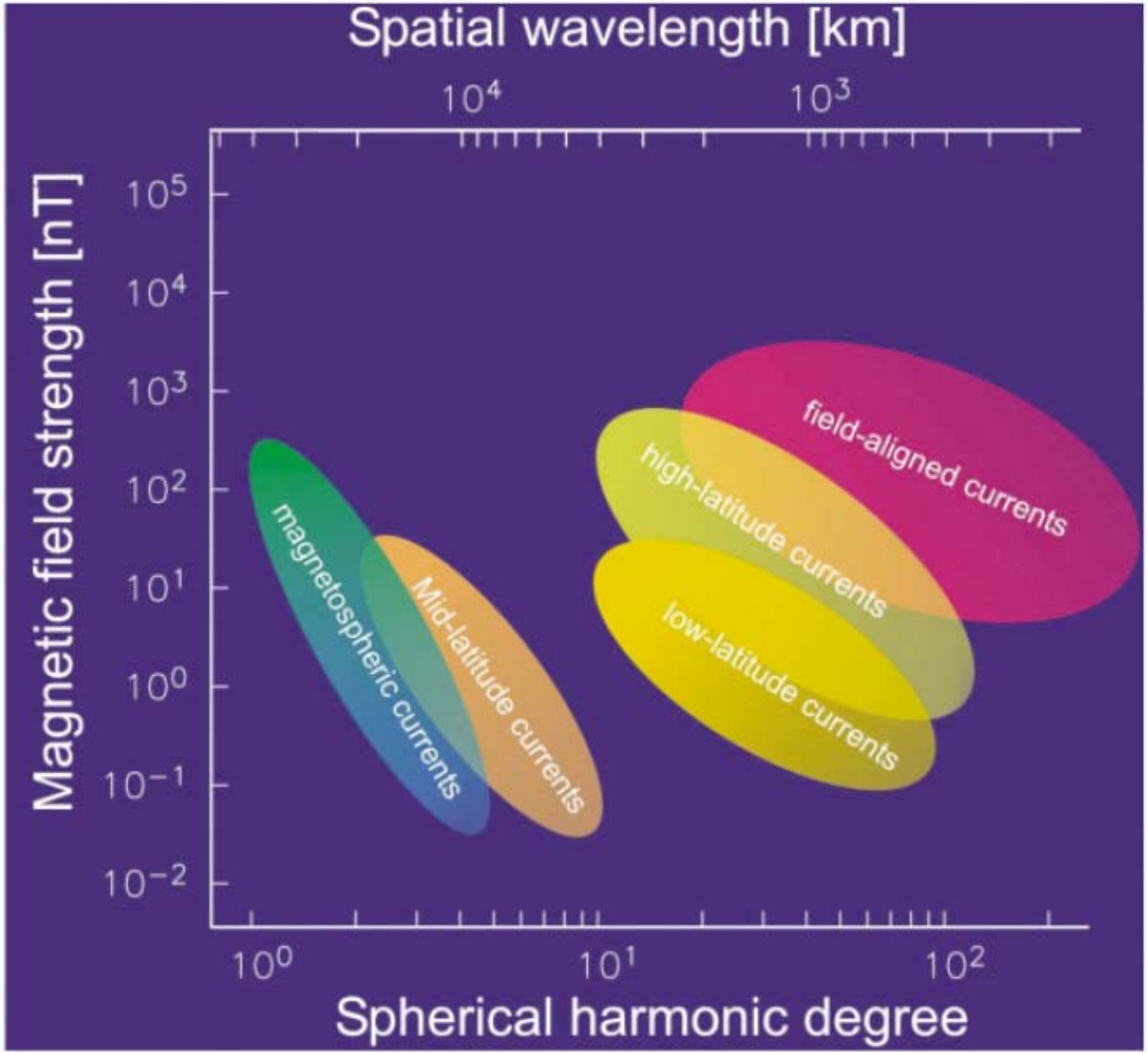

Signal amplitude at orbit altitude of the contributions from processes contributing to the magnetic field as a function of spatial scale. Source terms from external sources. From E. Friis-Christensen, H. Lühr, and G. Hulot, Earth Planets Space, 58, 351–358, 2006.

Experiments

Credit: ESA

Experiments

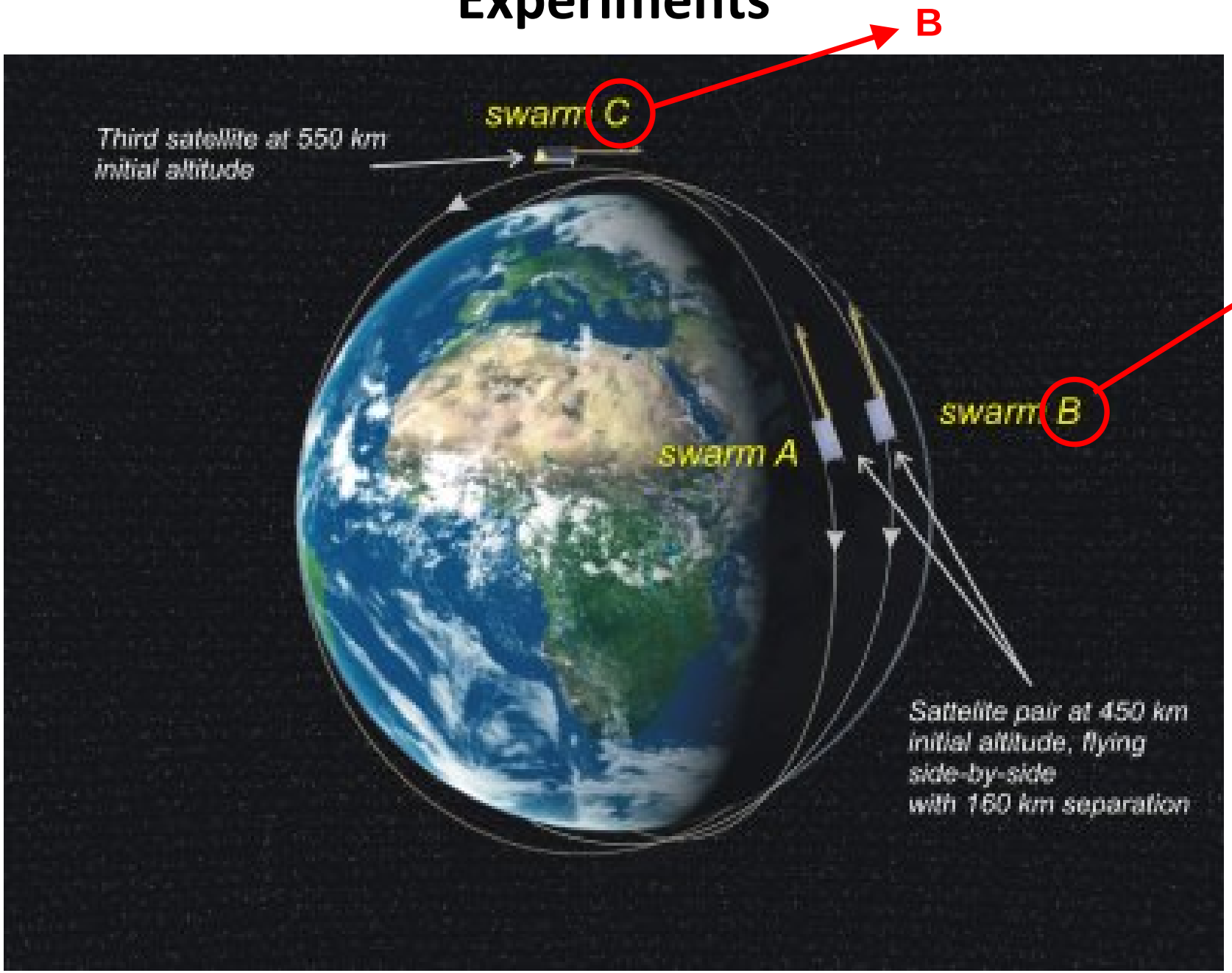

Credit: ESA

Experiments

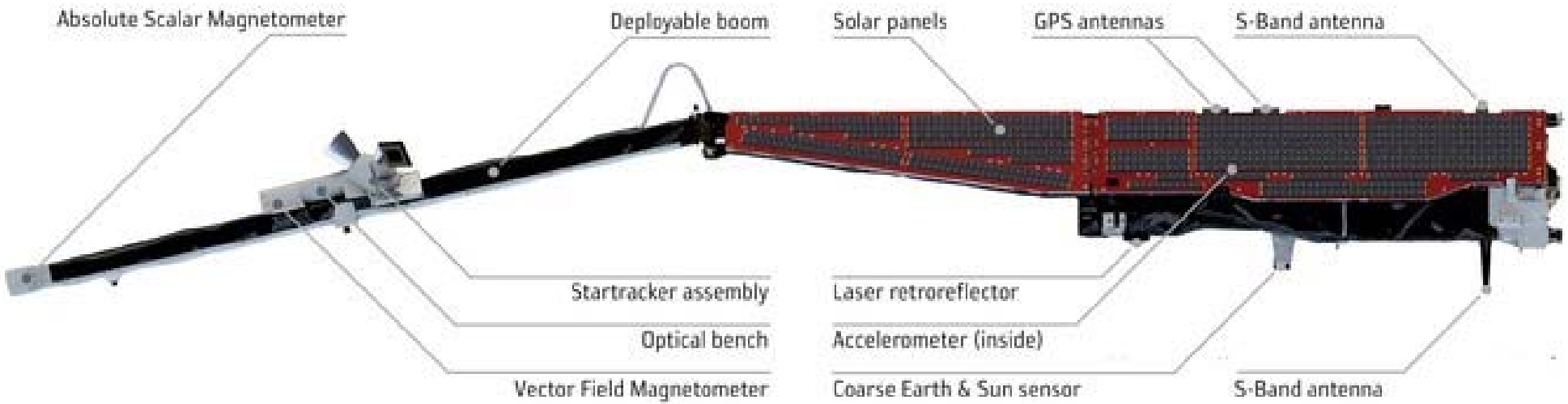

Credit: ESA

Experiments

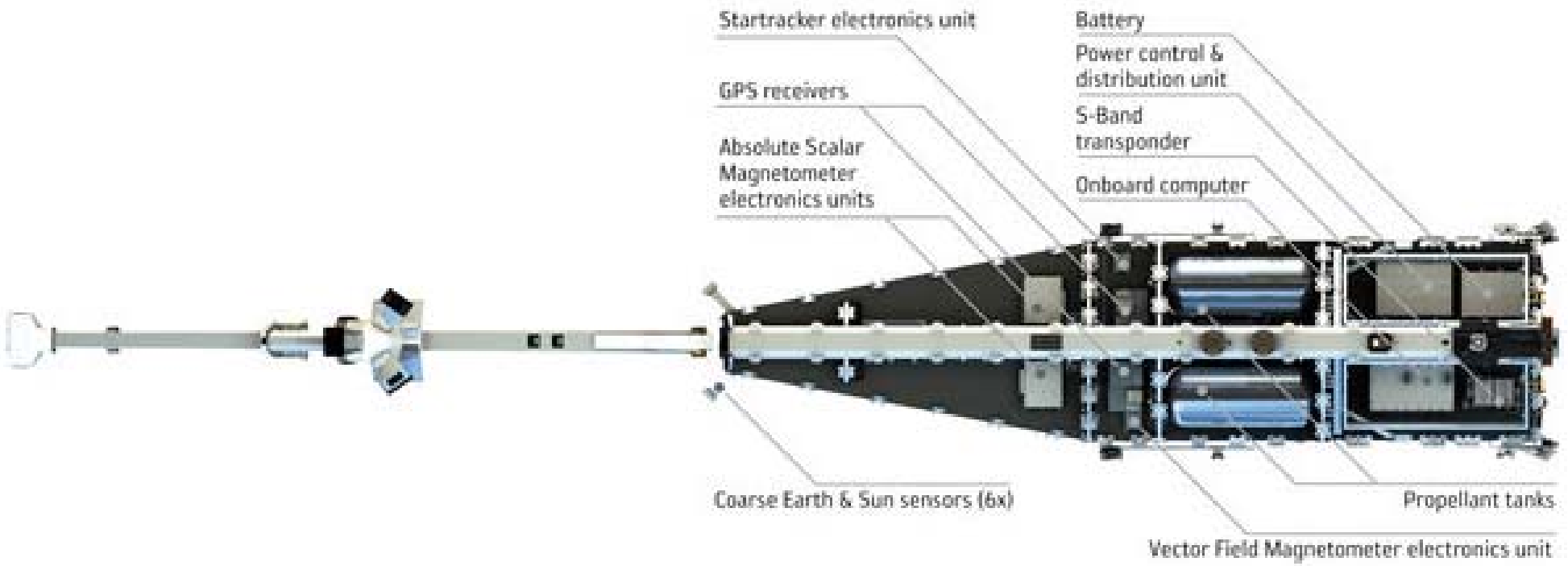

Credit: ESA

Experiments

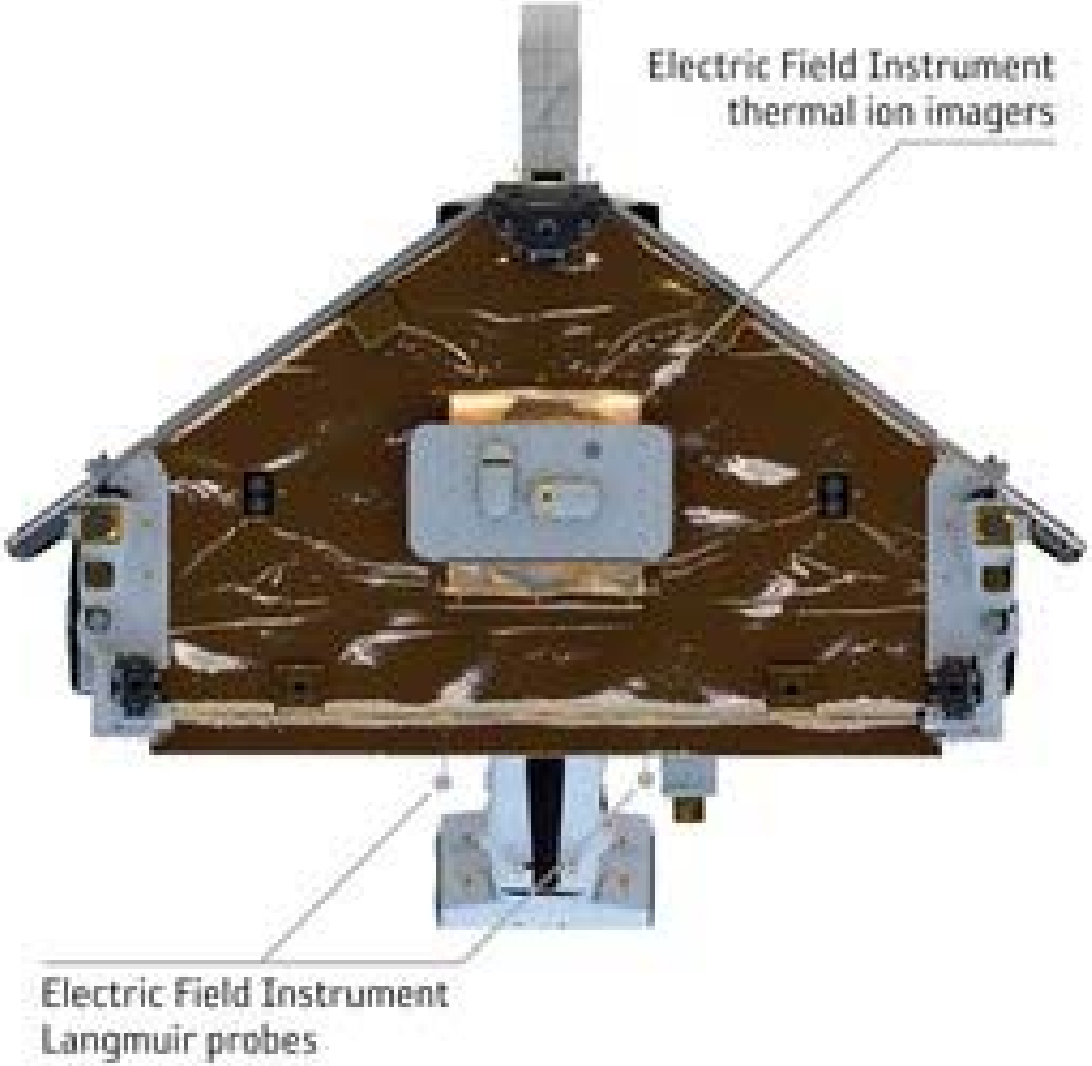

Credit: ESA

Current payload on board Swarm satellites

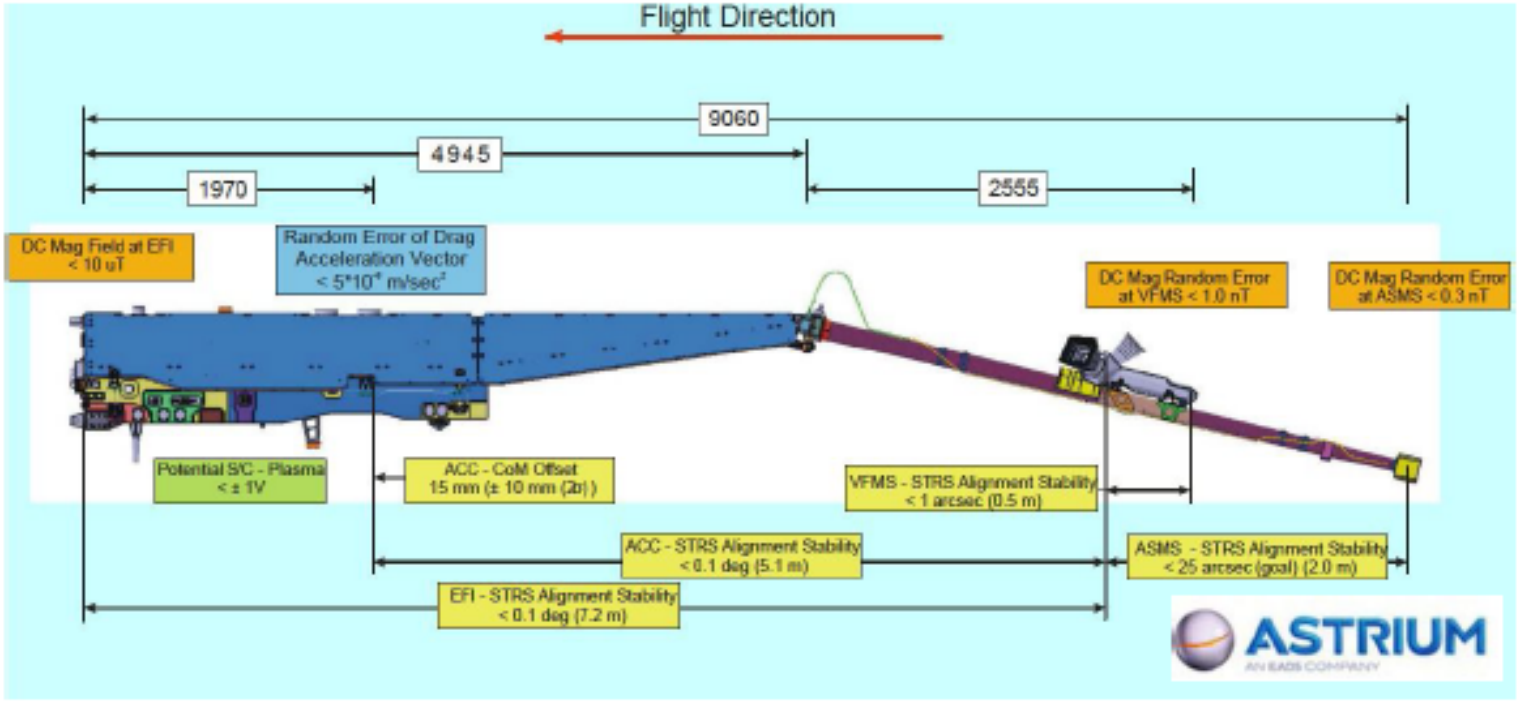

Absolute Scalar Magnetometer (CEA/LETI, CNES), 1Hz + 1Hz experimental vector data
Vector Field Magnetometer and Star Tracker (DTU Space), 50Hz, 1Hz
Accelerometer (VZLU, CZ), 1Hz
Electric Field Inst. (Charge particle imager, UC; Langmuir Probe, Uppsala), 2Hz
GPSR (Ruag), 1 Hz

Credit: Hulot et al., Swarm Delta, 5th Swarm DQW, Paris, Sep. 2015

CalVal Activities

- Magnetic field (VFM, ASM)
  - VFM-ASM residuals (< 1nT)
  - Mapping of ASM swA to swC (~1 nT)
- Electric field (TII, LP)
  - TII image: baseline vs. s/c potential; temperature…
  - TII: 4 orbits swA, 2 orbits swB, 1/4 orbit swC
  - LP: low gain vs high gain; s/c potential? ; e- temperature?
- Neutral density & winds (ACC, GPS)
  - Spikes & jumps in ACC data (temperature effects?)

CalVal Activities - TII

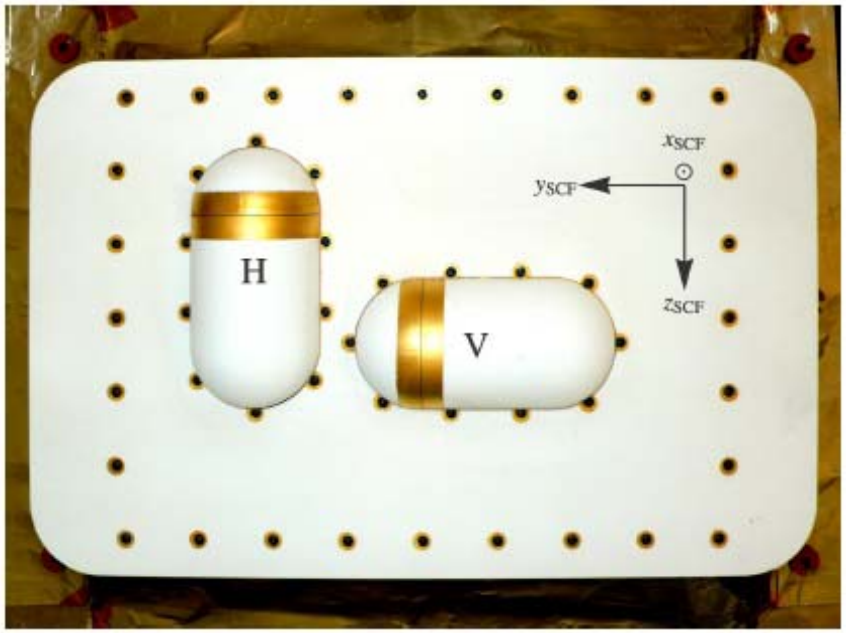

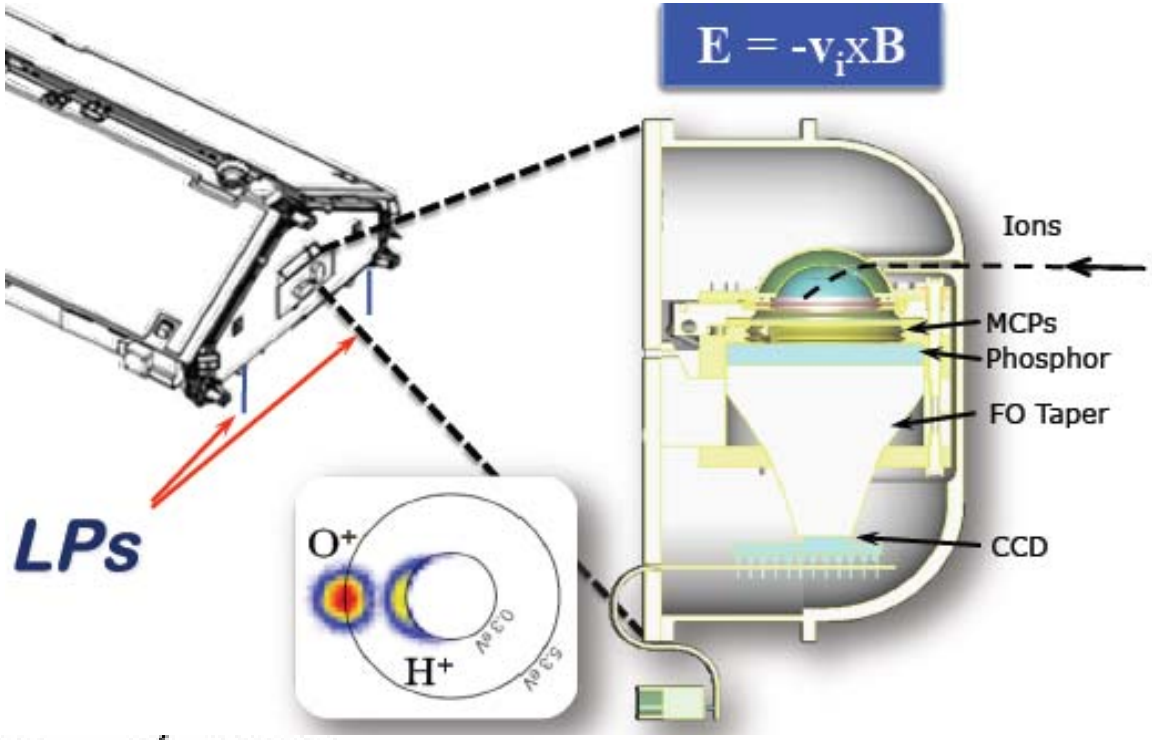

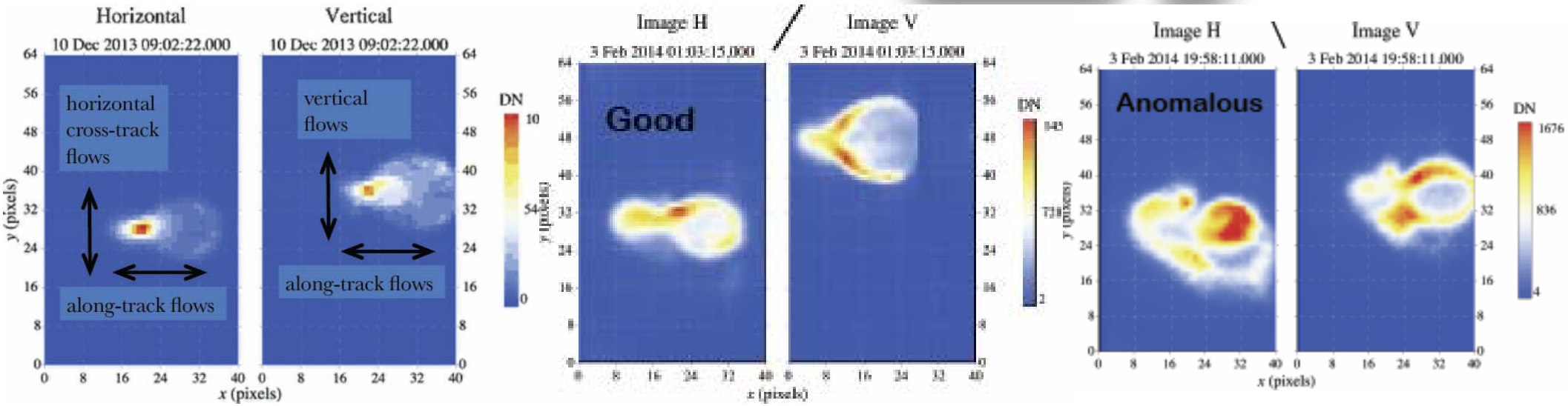

D. Knudsen, J. Burchill, Swarm 5th DQ Workshop, Paris, Sep. 2015

Data Products

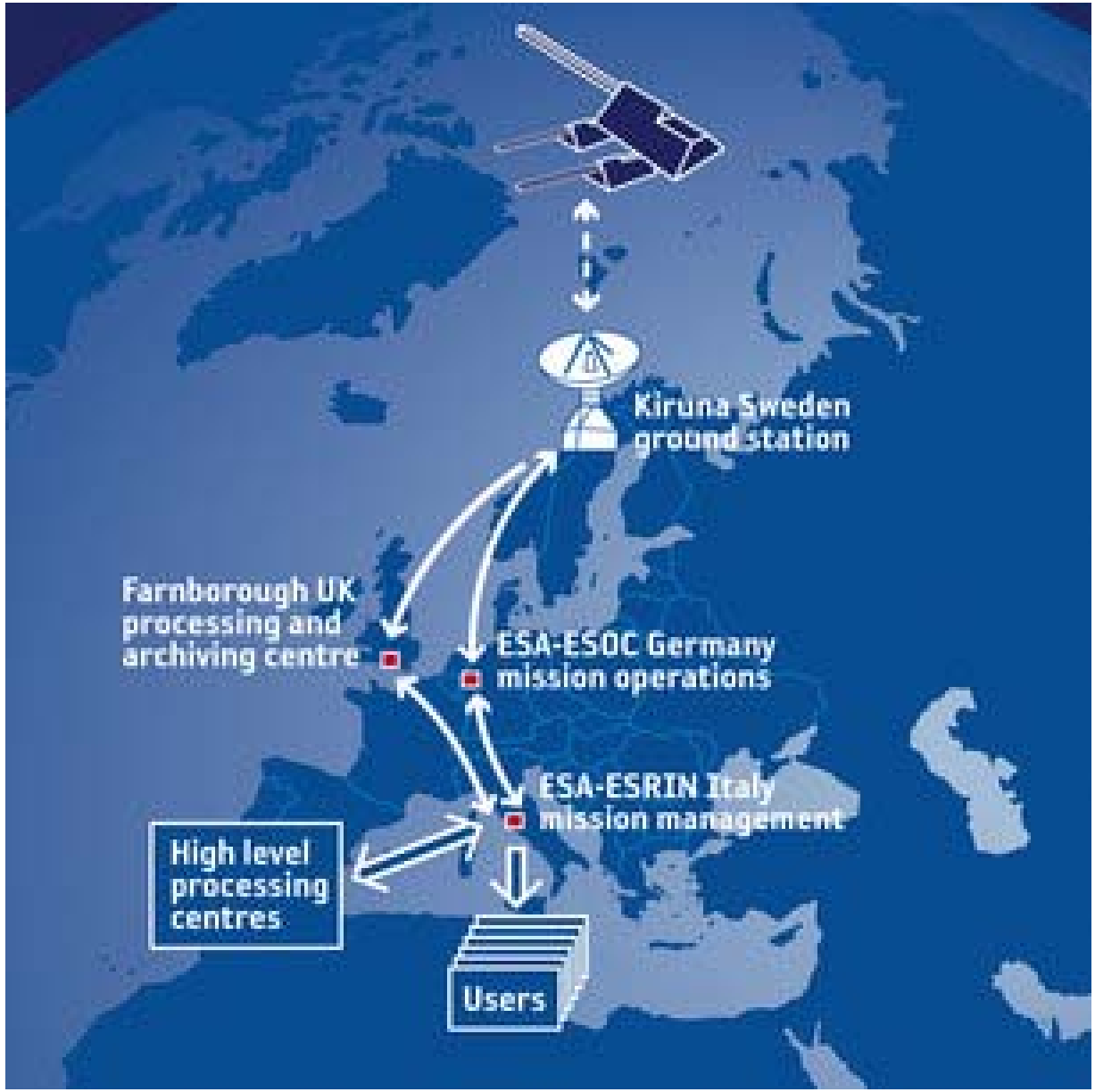

Credit: ESA

Data Products

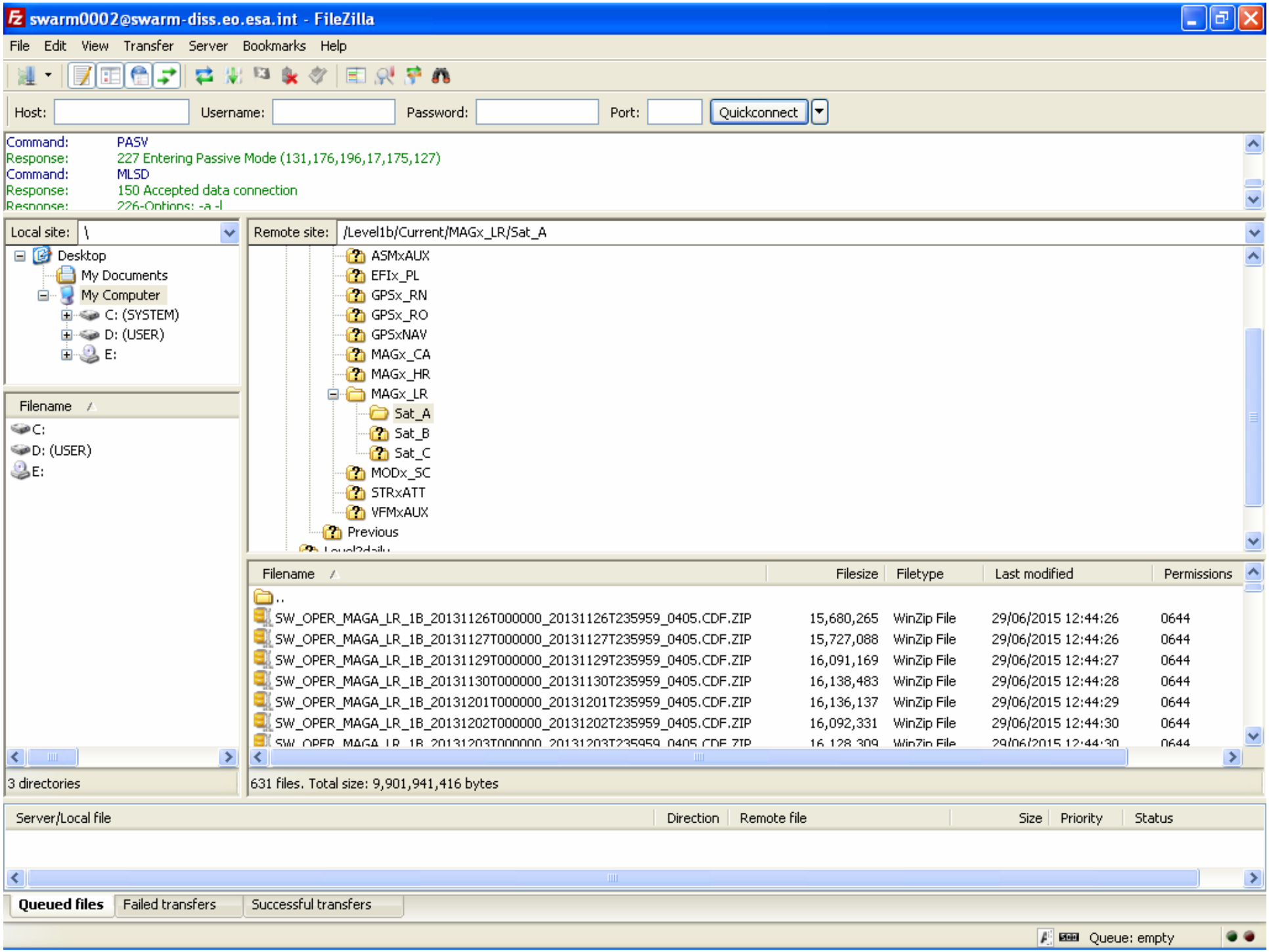

Highlights – Main magnetic field

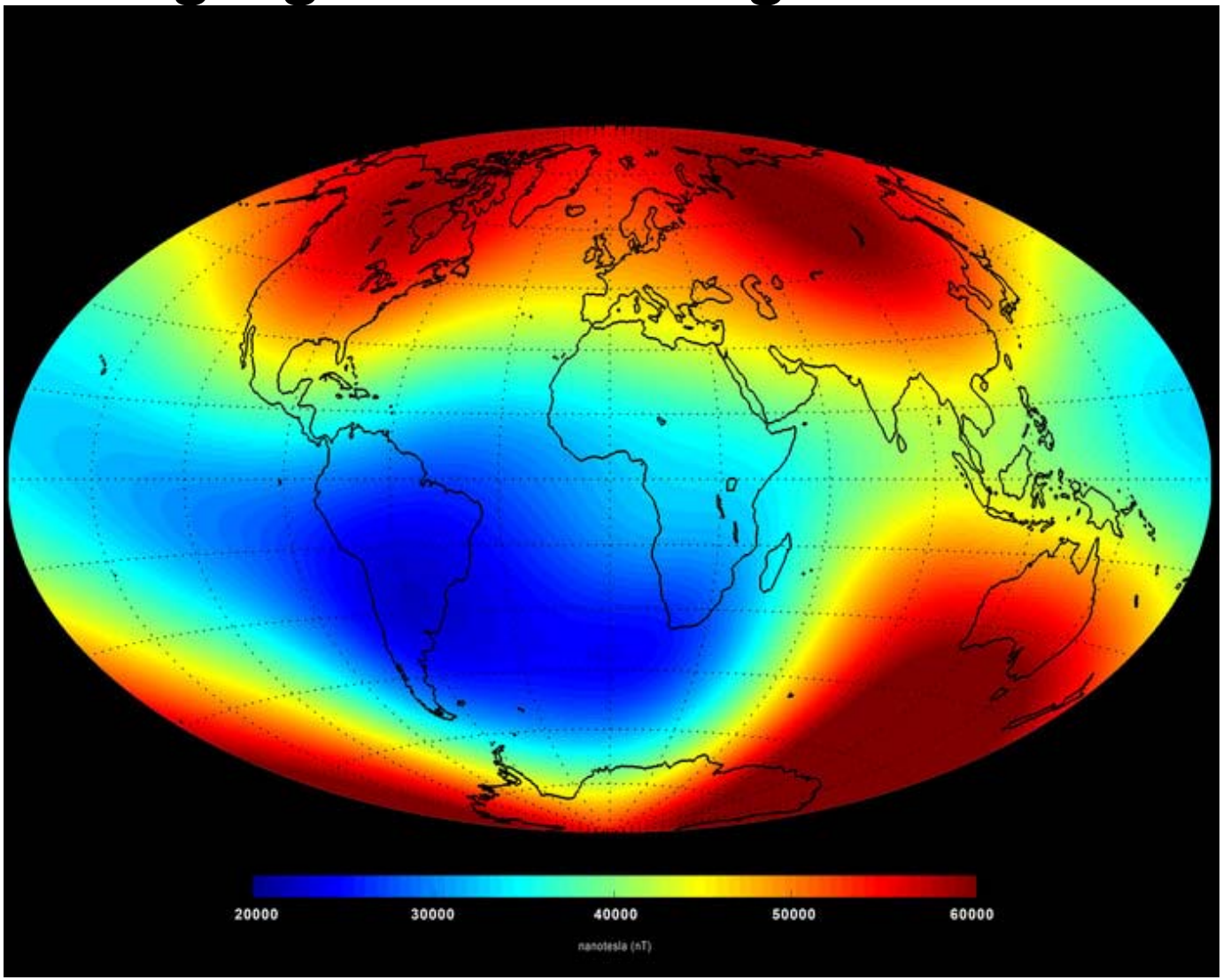

‘Snapshot’ of the main magnetic field at Earth’s surface as of June 2014 based on Swarm data. The measurements are dominated by the magnetic contribution from Earth’s core (about 95%) while the contributions from other sources (the mantle, crust, oceans, ionosphere and magnetosphere) make up the rest. Red represents areas where the magnetic field is stronger, while blues show areas where it is weaker. Credit: ESA.

Highlights – Magnetic field variation

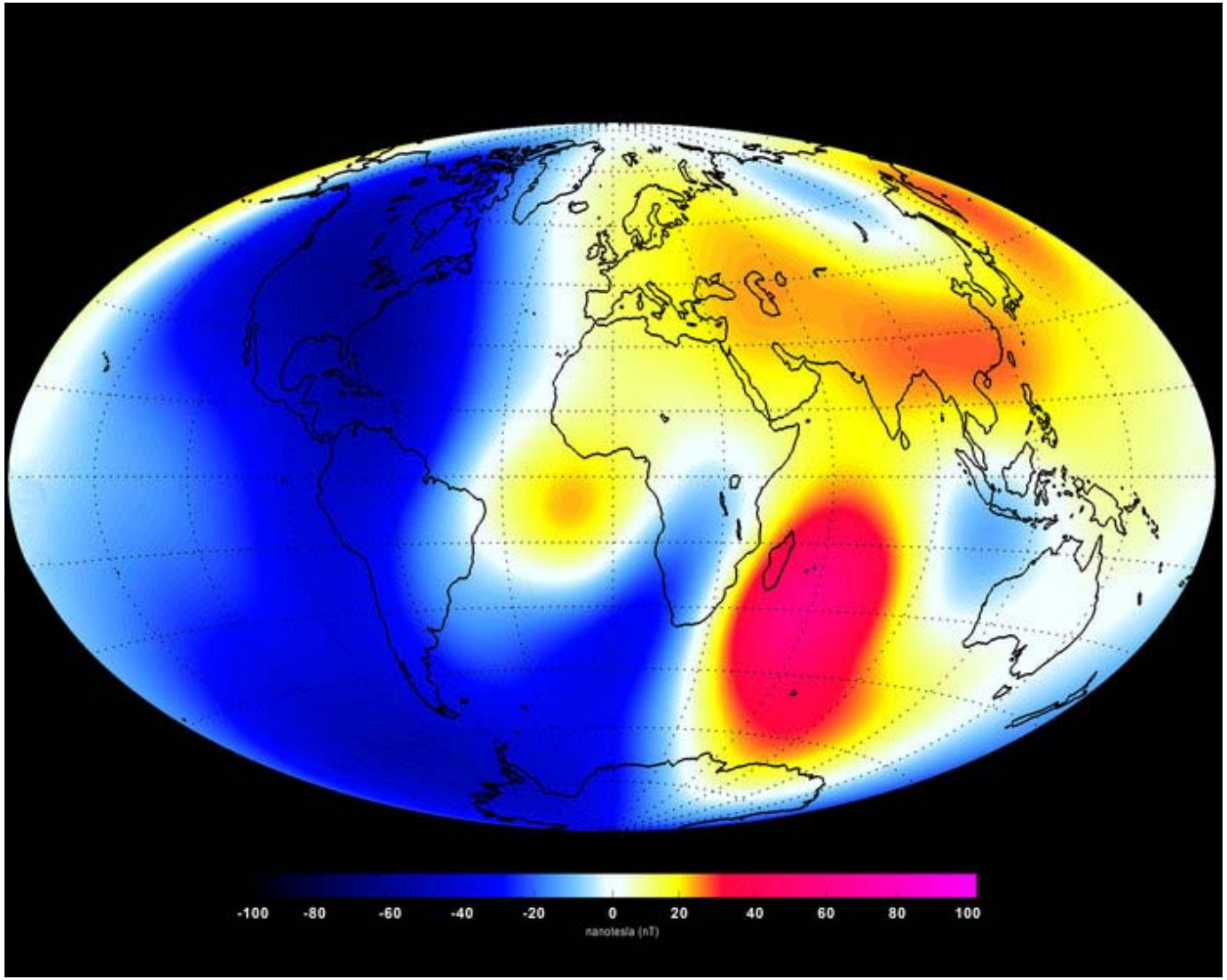

Changes in Earth's magnetic field from January to June 2014 as measured by the Swarm constellation of satellites. These changes are based on the magnetic signals that stem from Earth's core. Shades of red represent areas of strengthening, while blues show areas of weakening over the 6-month period. Credit: ESA

Highlights – Crust and core magnetic field

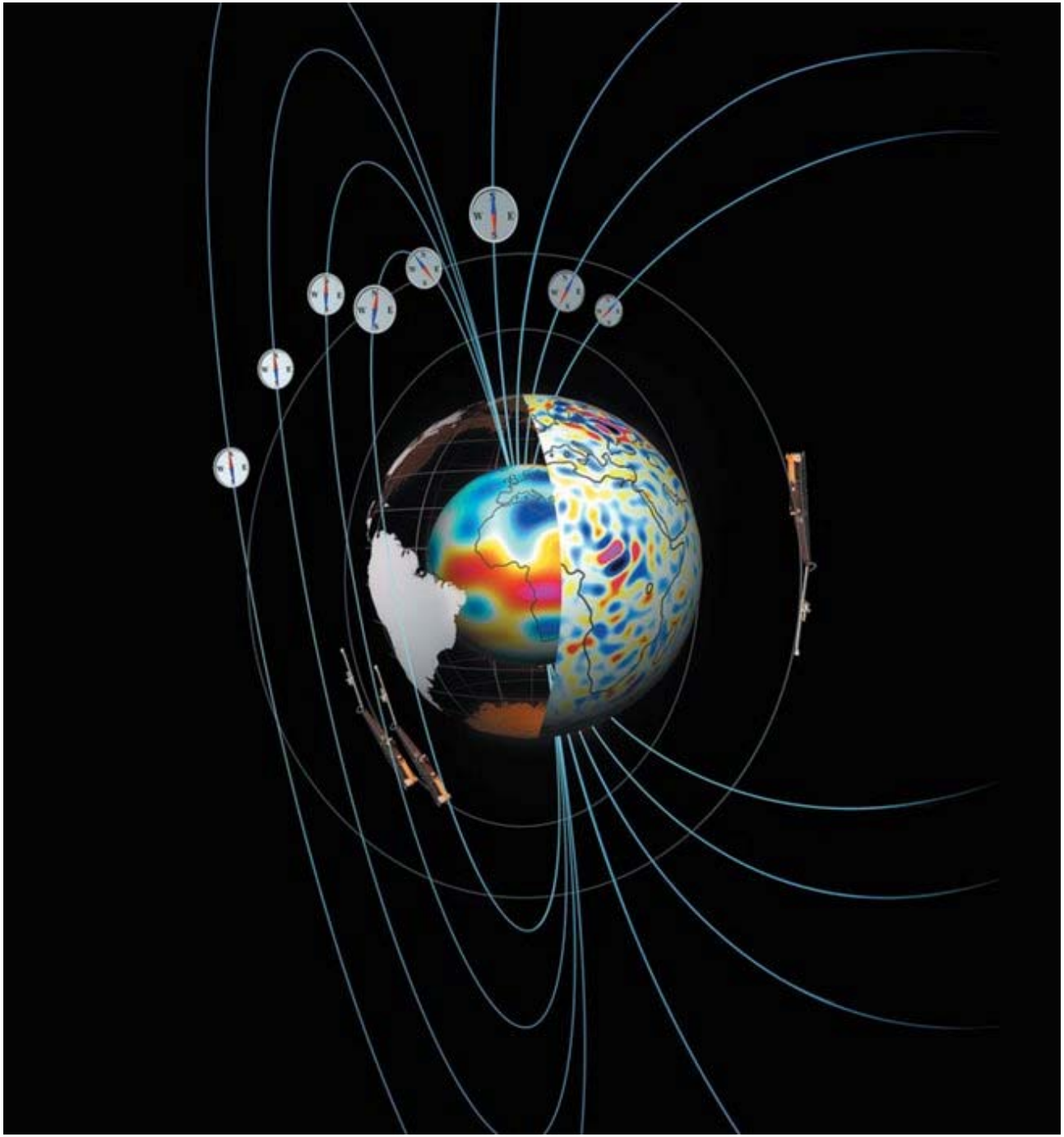

The image highlights the new crust (right) and core (centre) magnetic field models from Swarm. These preliminary results are based only on the first year of data.

Highlights – Mantle Conductivity

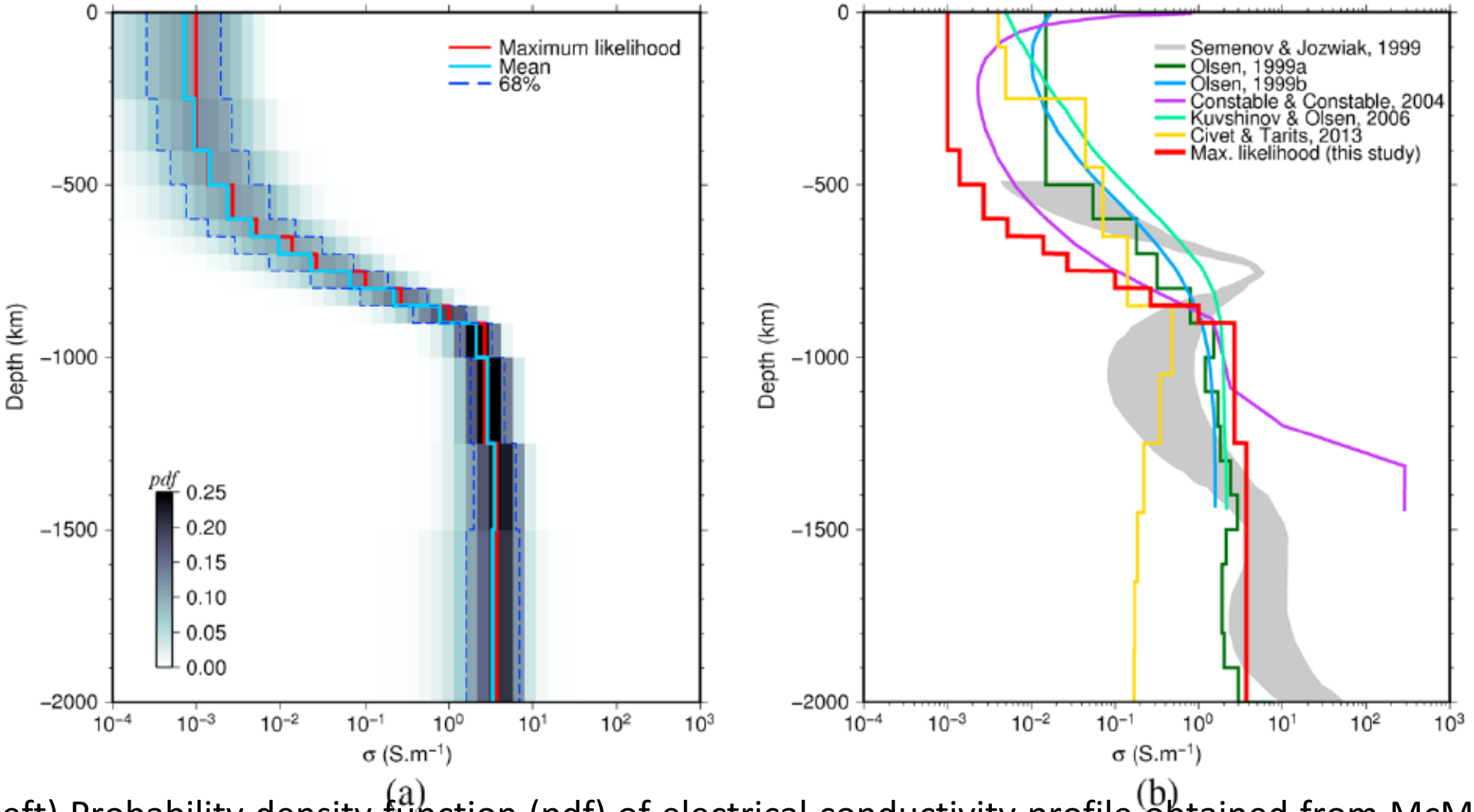

(left) Probability density function (pdf) of electrical conductivity profile obtained from McMC inversion of Swarm L1b data. The maximum likelihood (red) and the mean value (plain blue) with 1 standard deviation error bar (dashed blue) are also represented. (right) Maximum likelihood of the McMC pdf (red) compared to previous studies [Semenov and Jozwiak, 1999; Olsen, 1999a, 1999b; Constable and Constable, 2004; Kuvshinov and Olsen, 2006; Civet and Tarits, 2013]. From Civet et al., GRL Swarm Special Section, 2015.

Highlights – Equatorial Electric Field

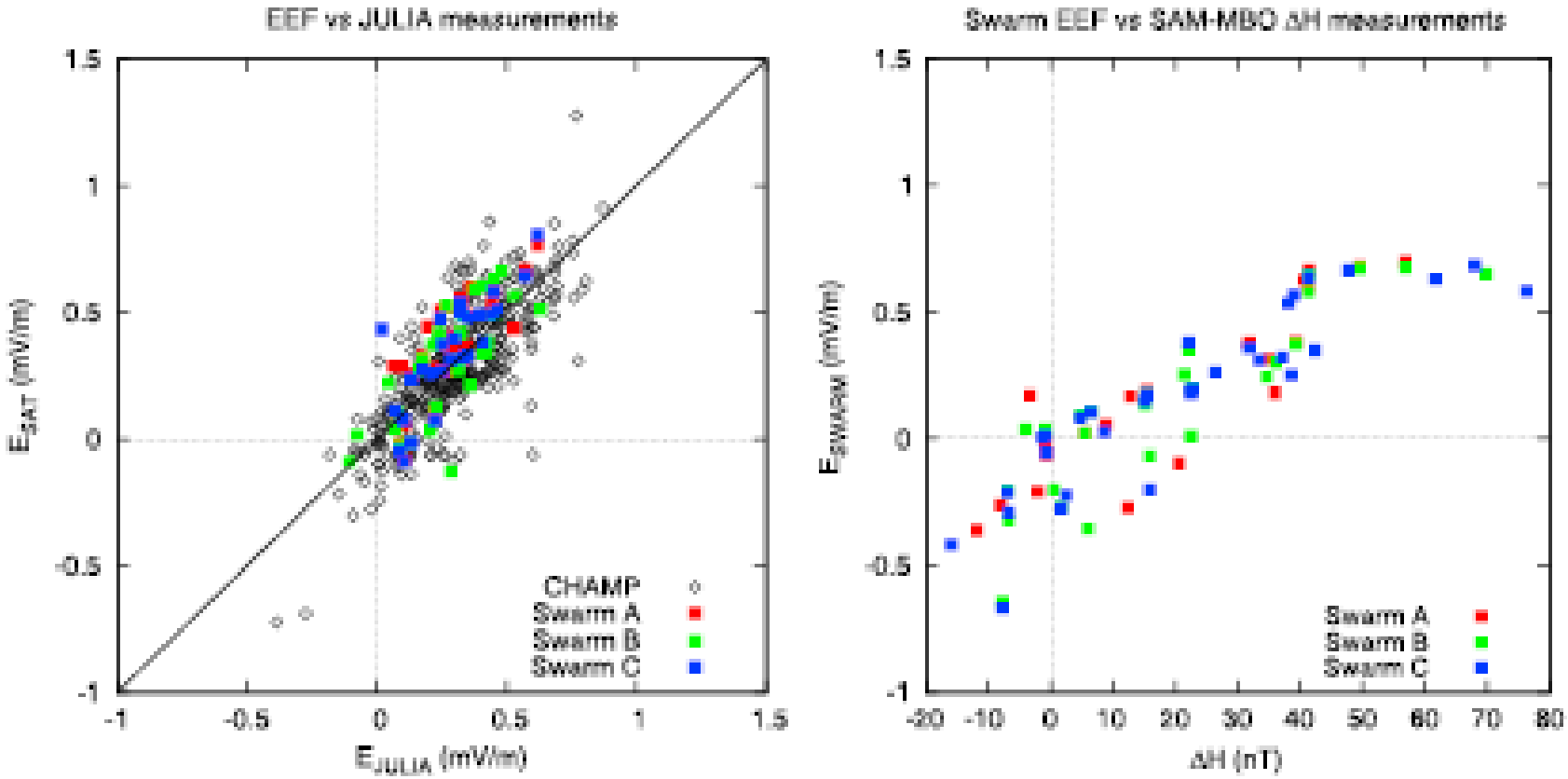

Figure 4. (left) Comparison of JULIA electric field measurements with CHAMP-derived EEF (2000–2010) and Swarm-derived EEF (November 2013 to October 2014); $y = x$ line shown as solid. (right) Comparison of Swarm-derived EEF with WAMNET SAM-MBO ΔH measurements.

Alken et al., GRL Swarm Special Section, 2015.

Highlights – ULF Pc3

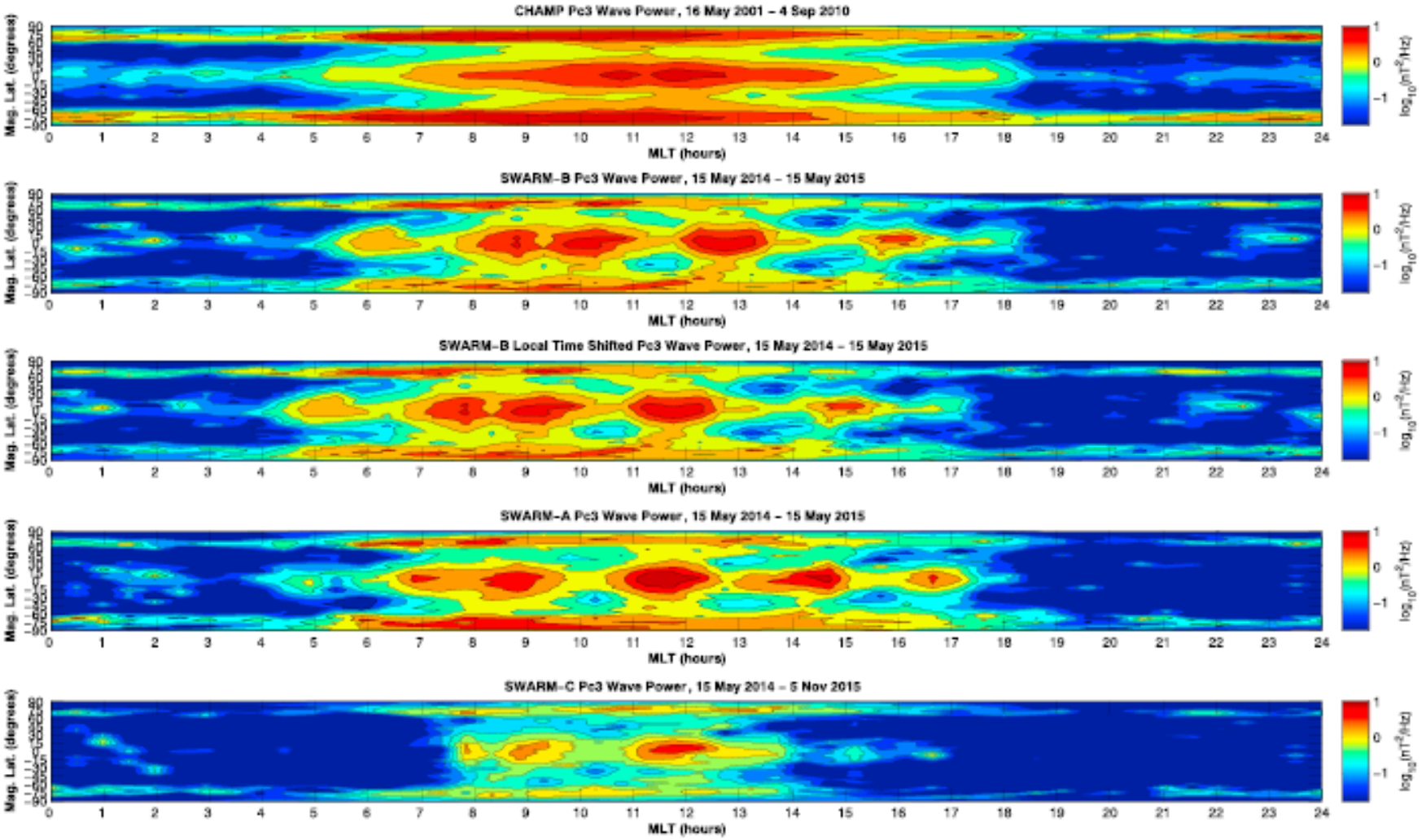

Figure 3. Mapping of the location of detected ULF wave activity on the magnetic latitude versus MLT space. Colors indicate the summed wave power per second at each point. (first panel) CHAMP (450–300 km), Swarm B (~ 510 km) (second panel) unshifted and (third panel) shifted by an hour in MLT, (fourth panel) Swarm A (~ 460 km), and (fifth panel) Swarm C (~ 460 km). We note that Swarm C has about half a year less observations than B and A.

Balasis et al., GRL Swarm Special Section, 2015.

Highlights – Temperature anisotropy

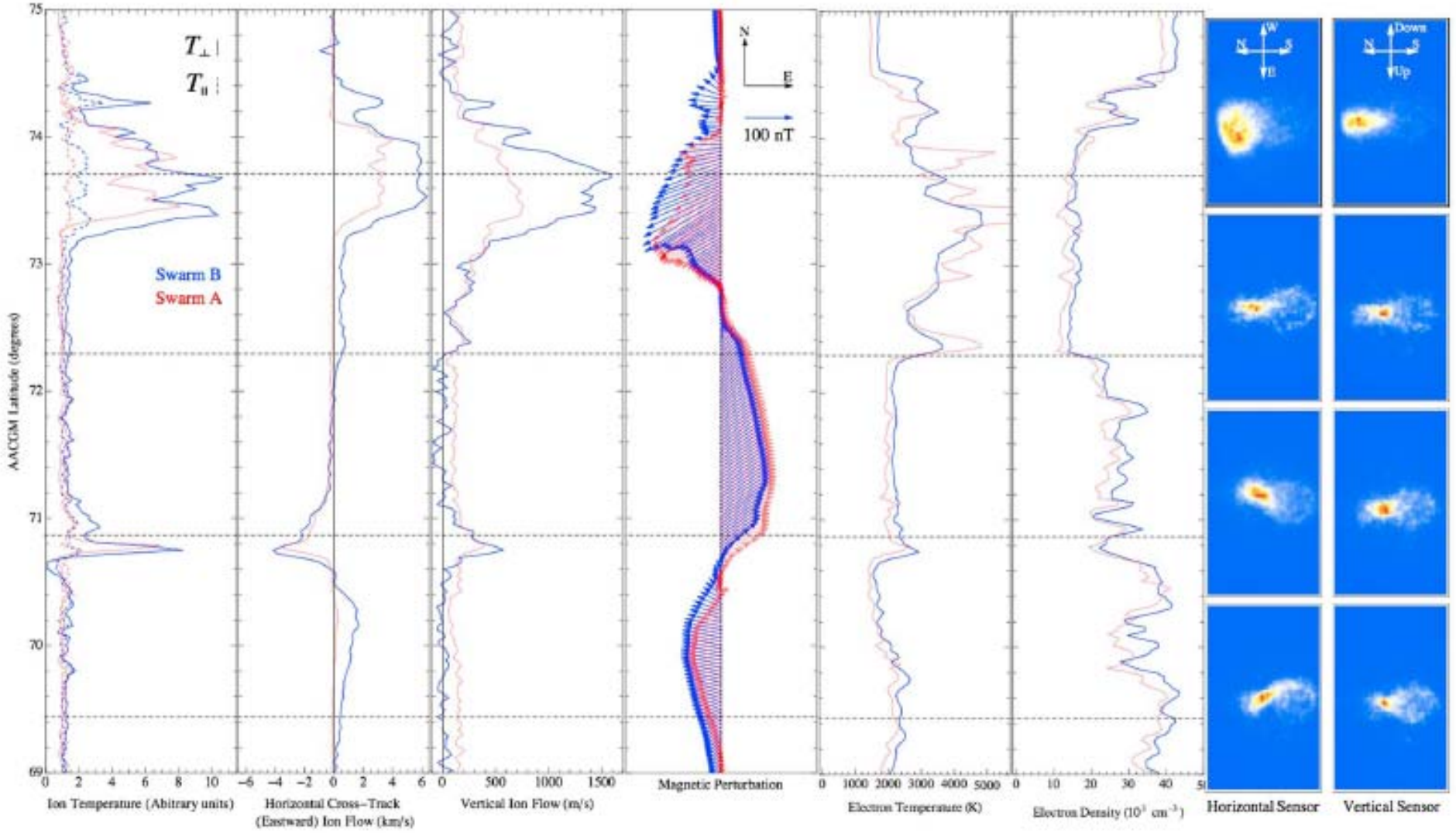

Figure 2. Anisotropic heating event observed by the Swarm B (blue) and again by Swarm A (red) roughly 30 s later. Ion temperature, horizontal flow, upward flow, and horizontal/vertical sensor images were measured by the TII. Magnetic variations were determined using the Vector Field Magnetometers (VFM). Electron temperature and electron density were measured by the Langmuir probe. TII raw images were taken coincident with dashed black lines. Swarm B was traveling antisunward around 01:42 MLT on 13 December 2013 between 04:52:05 UT and 4:54:46 UT.

Archer et al., GRL Swarm Special Section, 2015.

Highlights – Swarm/Cluster conjunction

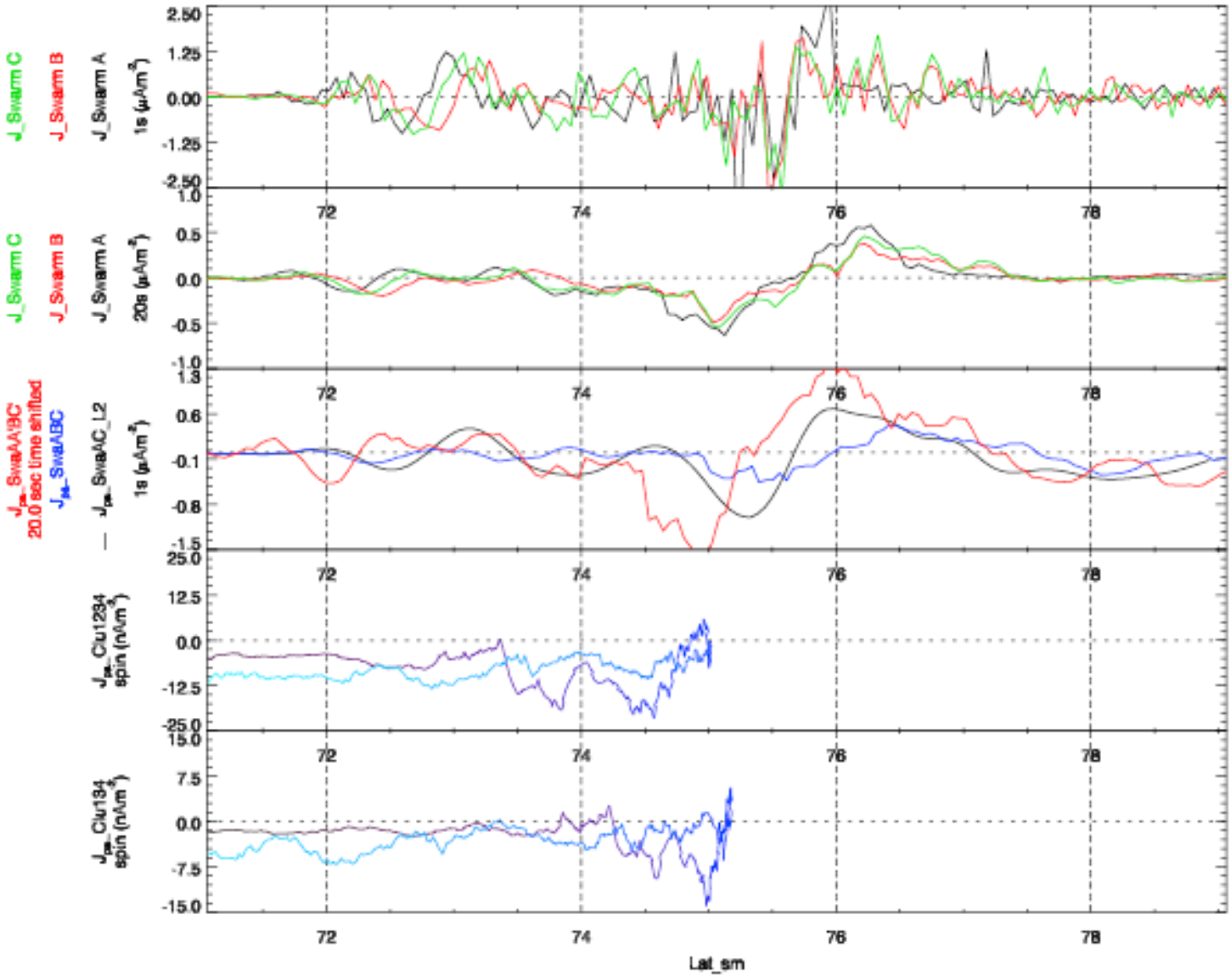

Figure 5. Mapped MLAT (in SM coordinates) values of Swarm and Cluster FACs. The top three panels correspond to the same set of FAC estimates as shown in the top set of panels in Figure 5. The bottom two panels show the Cluster FACs estimated by the full curlometer and from one face formed by C1, C3, and C4 (as in the bottom two panels of Figure 4).

Dunlop et al., GRL Swarm Special Section, 2015.

ISS/JUB: Field-aligned currents

Three-S/C validation of ESA L2 FAC product

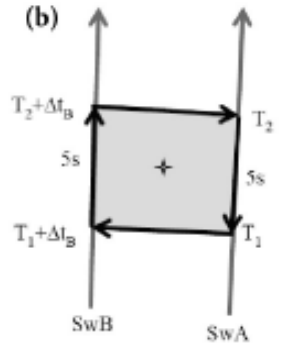

Ritter and Luhr, 2009

The 2 S/C method from Ritter et. al. 2013

- boundary integral method designed to be applied for the lower Swarm pair flying side-by-side
- -combines along-track with cross-track measurements to form virtual quads
- assumes linear field variation and time stationary

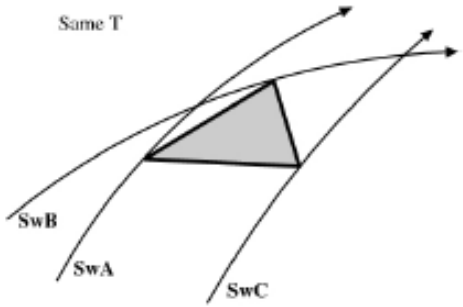

$$\nabla_n = \hat{\boldsymbol{n}}(\hat{\boldsymbol{n}} \cdot \nabla) \equiv \hat{\boldsymbol{n}} \frac{\partial}{\partial n}$$

$$\nabla_p = \nabla - \nabla_n$$

Vogt et al. , Ann. Geophys. 27, 2009

The 3 S/C method from Vogt et al., 2009

- developed for analyzing Cluster data
- from three points of observation, the planar gradient comp. can be obtained, enough to fully construct the normal component of the curl
- assumes linear field variation
- time-stationary is not needed
- the missing part (gradient along the direction normal to the satellite plane) can be inferred if additional constraints are used
- the additional constraints can be geometrical (gradient parall. or perp. to a certain direction) or physical (J only along B, time-stationarity)

A. Blagau, J. Vogt, M. He, Swarm 5th DQ Workshop, Paris, Sep. 2015

ISS/JUB: Field-aligned currents

Three-S/C validation of ESA L2 FAC product

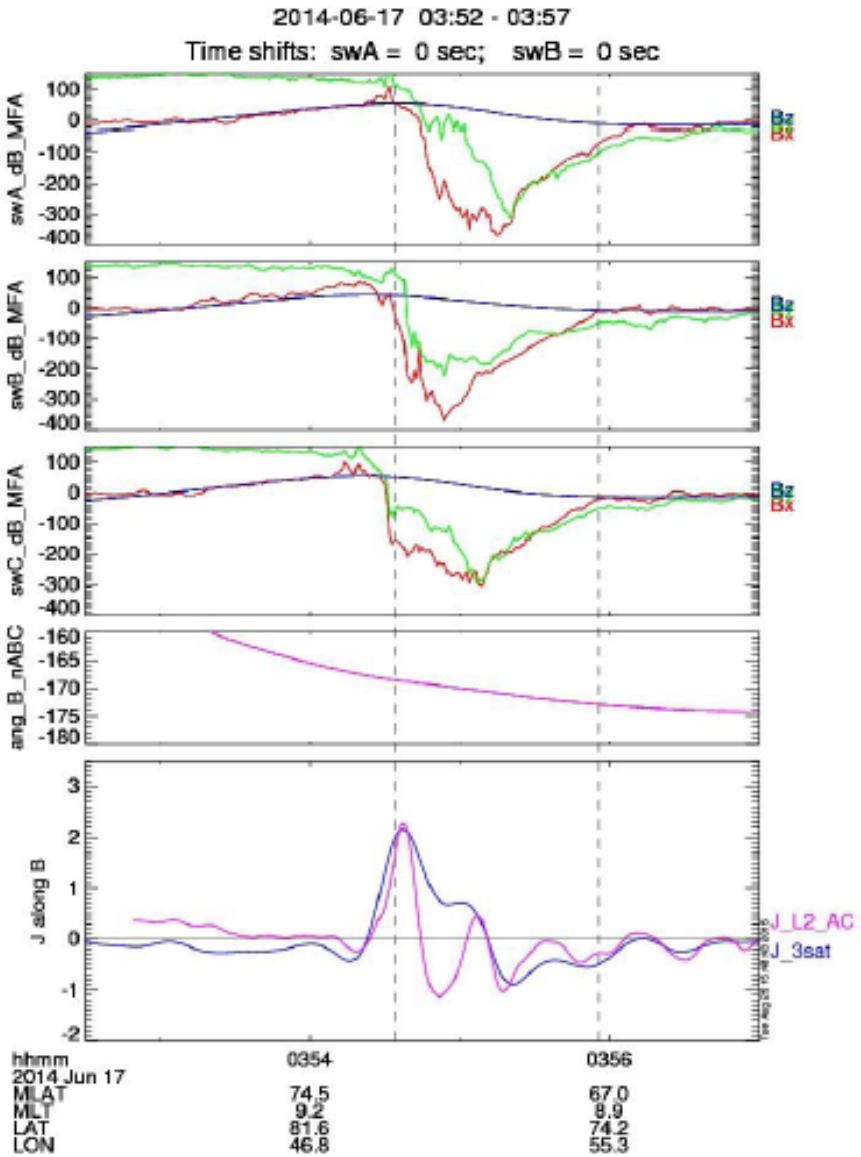

Event on 2014-06-17, ~03:55

Close separation: magnetic footpoint of SwB is between SwC and SwA.

Well-defined planar current sheet on all satellites (eigenvalue ratios: 6, 13, 15), *non-stationary*.

The FAC is within the methods' validity intervals: far from the exclusion zone (two-sat requirement) and main B field is far from the sat. plane (three-sat. requirement)

B model discrepancies: both L2 and our estimations are affected; visible in the FAC offset values at lower latitude =>for quantitative comparisons data detrending is needed.

A. Blagau, J. Vogt, M. He, Swarm 5th DQ Workshop, Paris, Sep. 2015

ISS/JUB: Field-aligned currents

Study of F-map impact on FAC calculation

Northern hemisphere

Average deviation in dB East component
Impact of Fmap calibration; Northern hemisphere

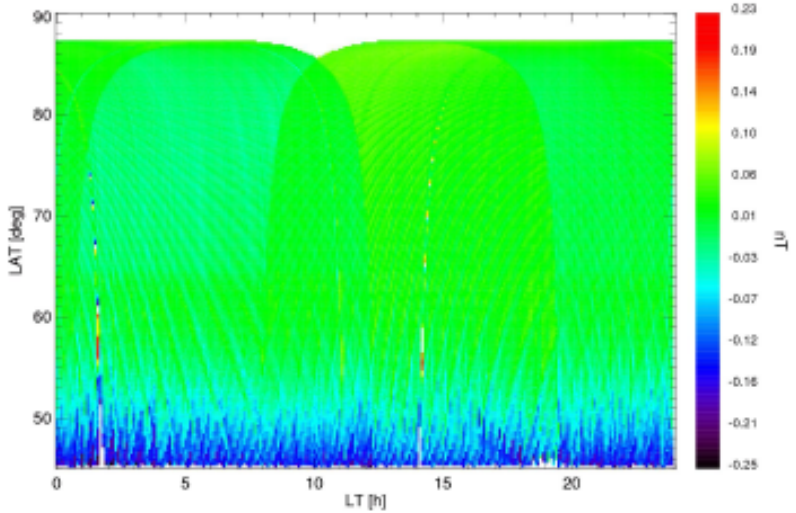

Standard deviation of dB East component
Impact of Fmap calibration; Northern hemisphere

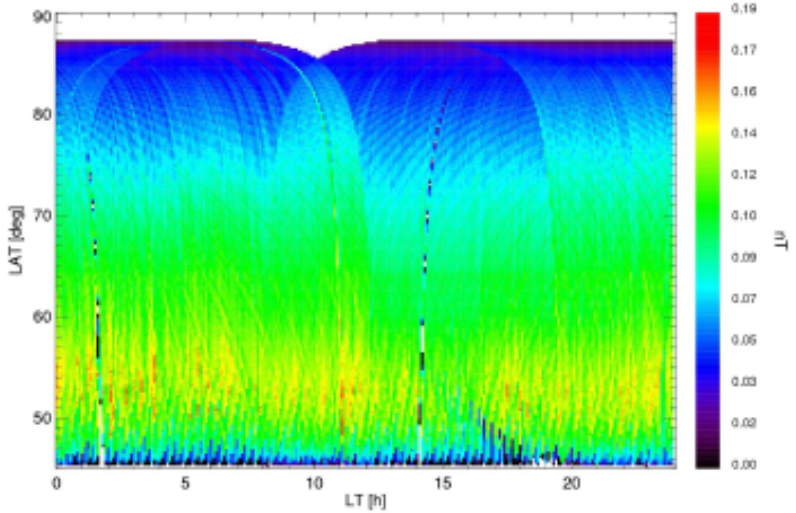

Southern hemisphere

Average deviation in dB East component
Impact of Fmap calibration; Southern hemisphere

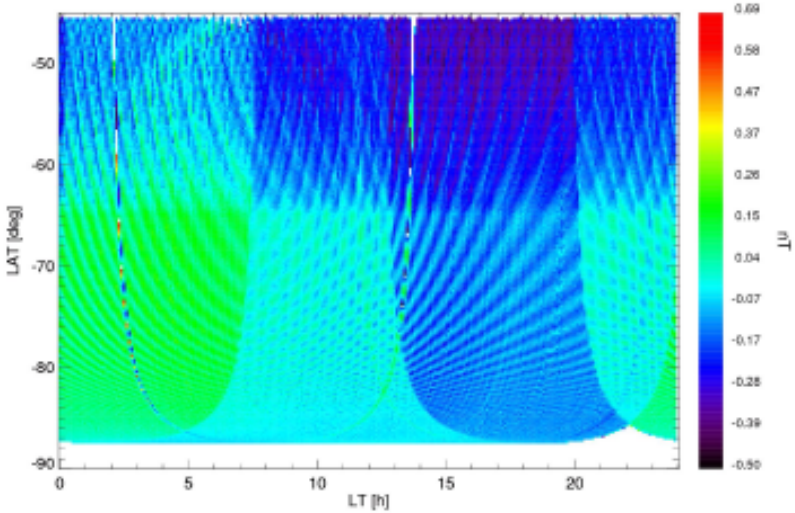

Standard deviation of dB East component
Impact of Fmap calibration; Southern hemisphere

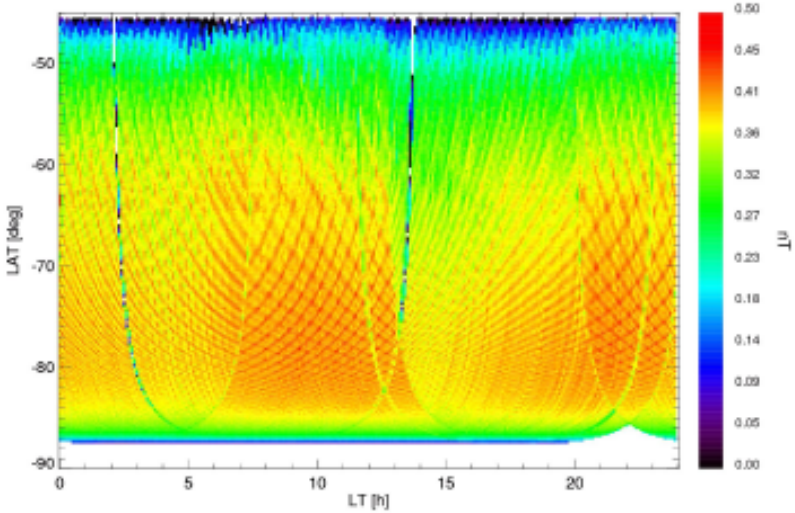

A. Blagau, J. Vogt, M. He, Swarm 5th DQ Workshop, Paris, Sep. 2015

ISS: Longitudinal Gradients

1D Arc ?

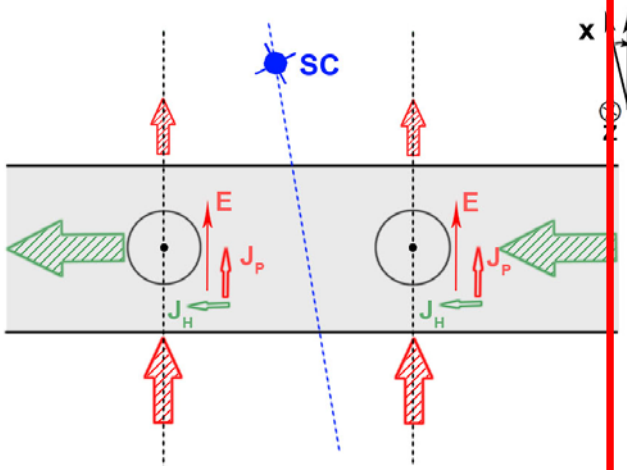

Quiet arcs in the evening and morning sectors, as well as the quiet auroral oval, can be approximated as 1D. In such cases, 1 s/c is enough to explore the arc / oval.

2D Arc ?

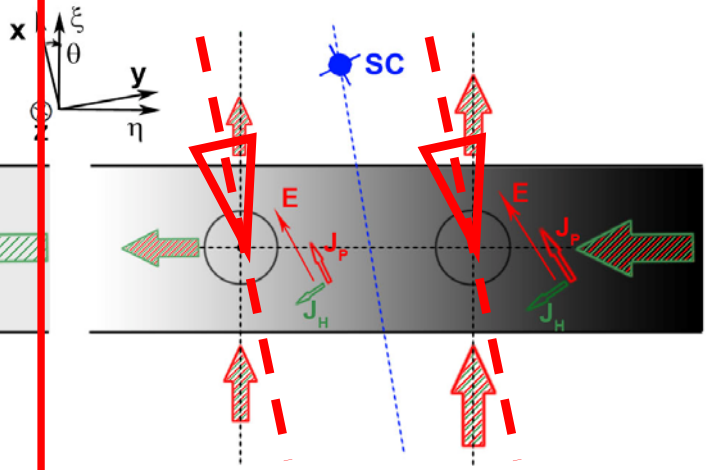

The 1D backbone can be extended by 2D features, like a divergent electrojet, whose local behaviour can still be explored by 1 s/c. However, data from 2 s/c are needed to check longitudinal gradients.

2D Aurora

A minimum of 3 s/c are needed to explore fully developed 2D aurora, ideally with conjugate radar data (conductance, electric field, neutral winds, etc).

Longitudinal Gradients – 1 vs 2 (or 3) s/c

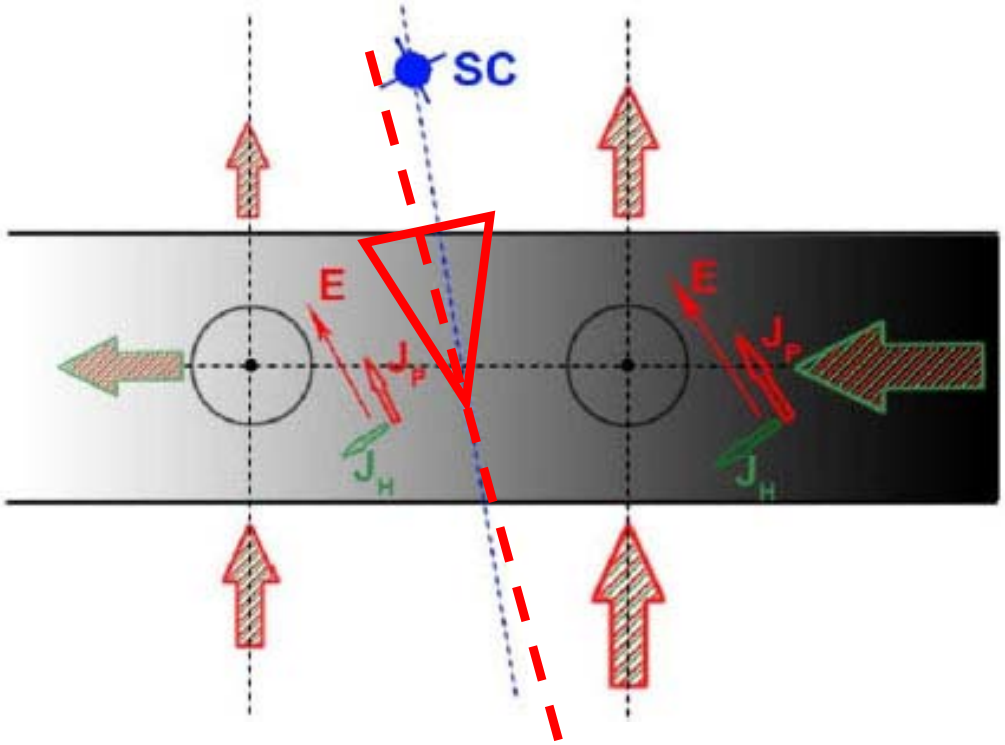

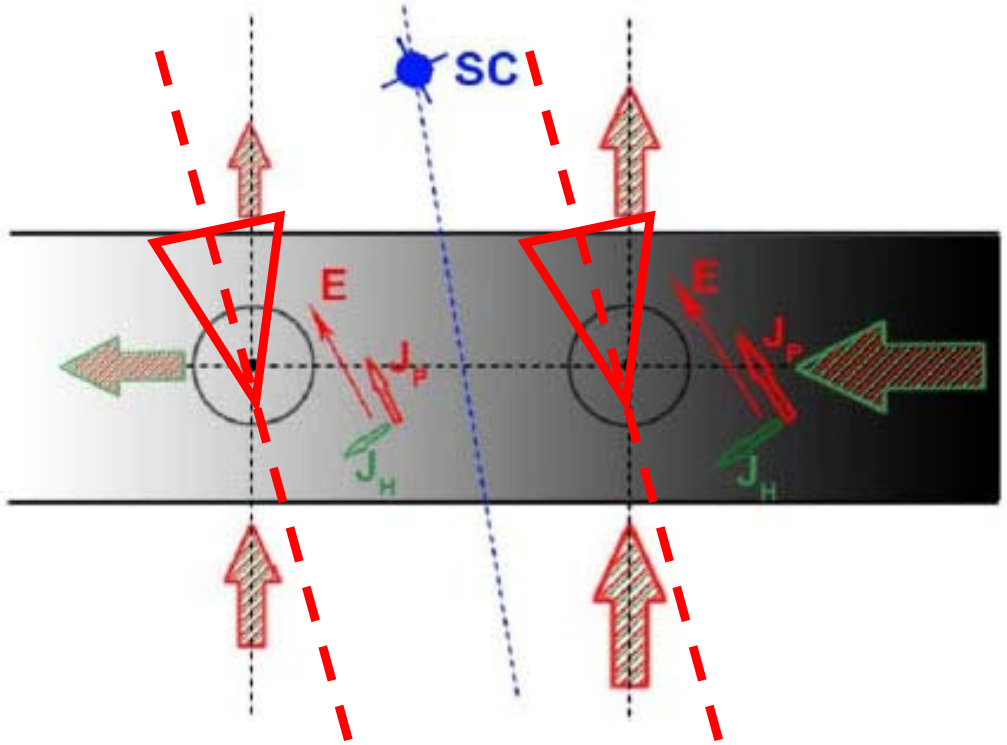

With 1 Swarm s/c:

- Compute the profile of Ex, depending on the **average Ex and Ey** (average cross-track and along-track velocity) and compare it with the (detailed) cross-track velocity.
- Derive the local divergence of electrojet currents
- **Conductance** is a key quantity, that can be derived from conjugate observations (radar, DMSP,…) and/or **Swarm 'conductance maps'.**

With 2 Swarm s/c:

- Compute longitudinal gradients in the field-aligned current and electric field.
- Compare local estimates of the electrojet divergence with the 'overall' divergence, based on 2 s/c.

With 3 Swarm s/c:

- Multi-scale investigations?

Bonus

- Address also the equatorial electrojet?

ISS/FMI: Electric field validation

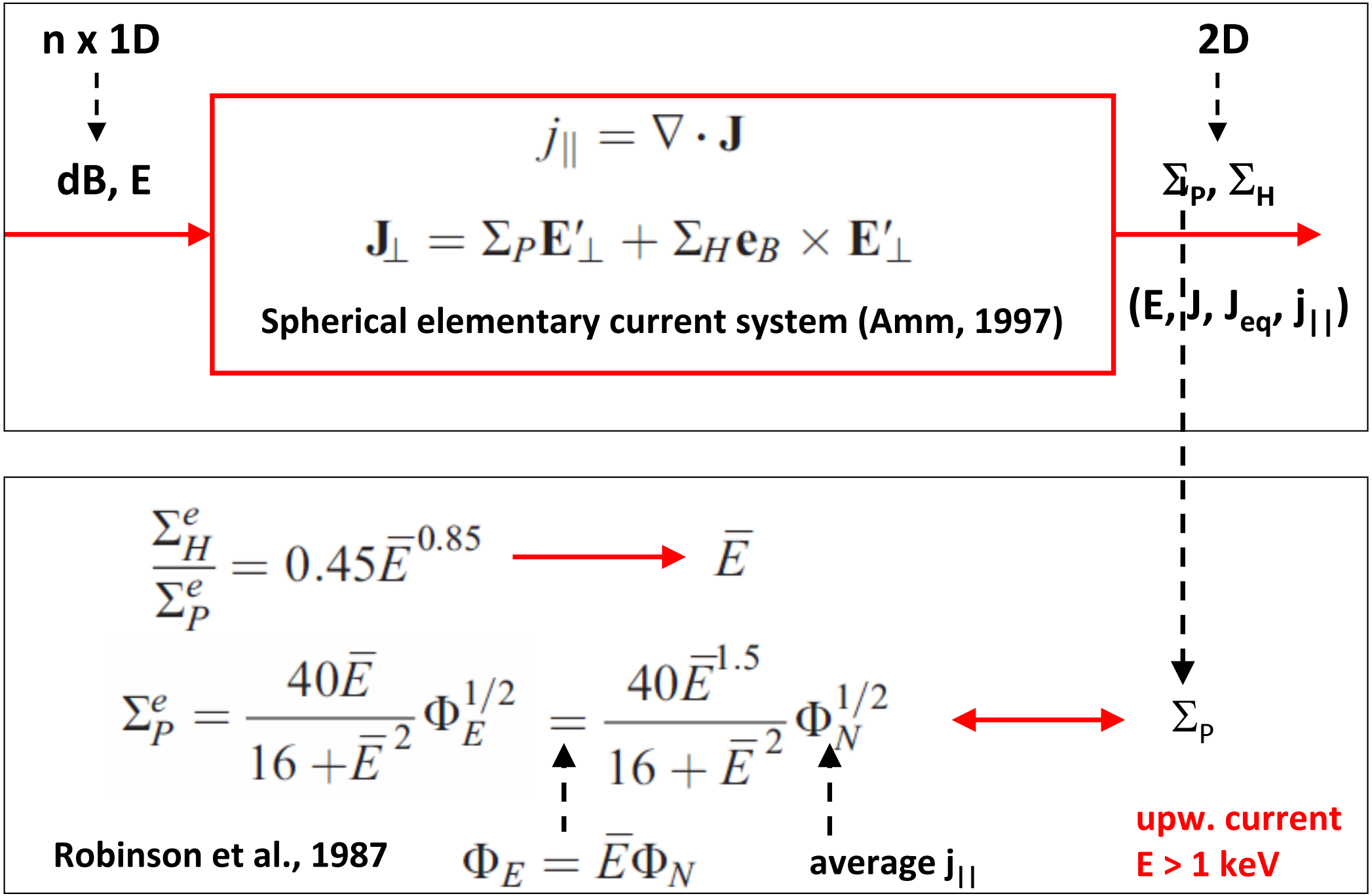

B. Event Selection – 3 s/c, ground data

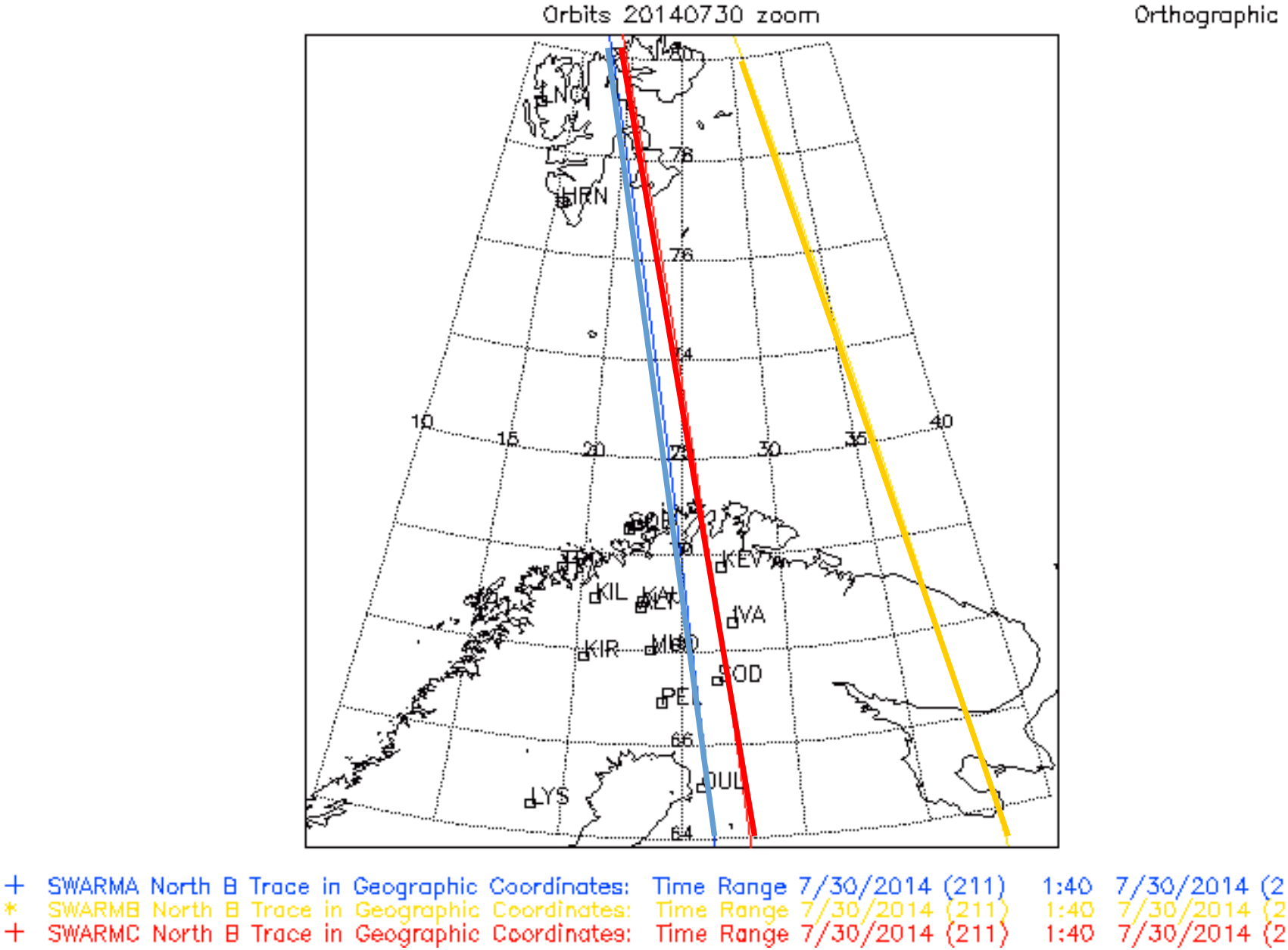

B. Event Selection – approx. 1D

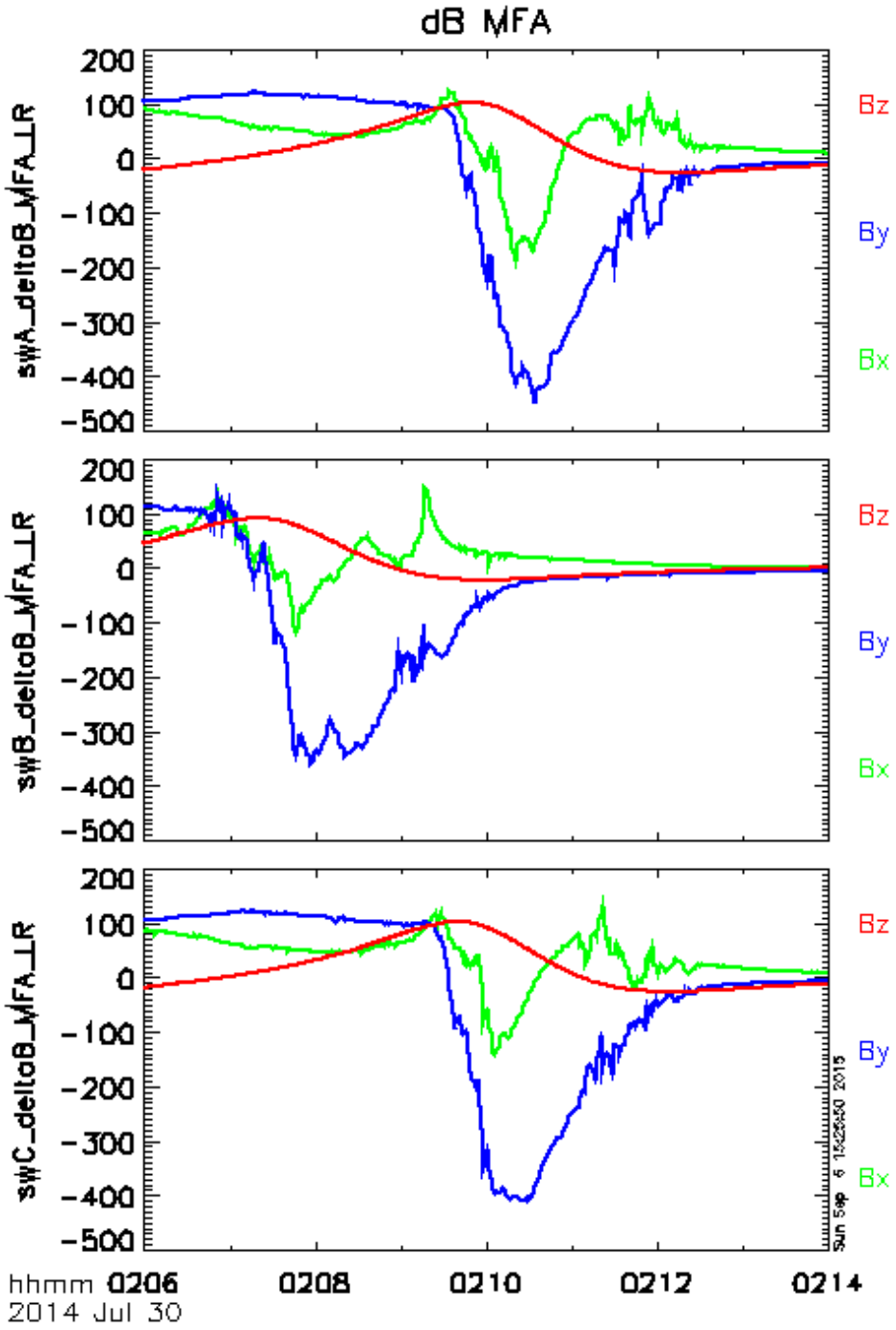

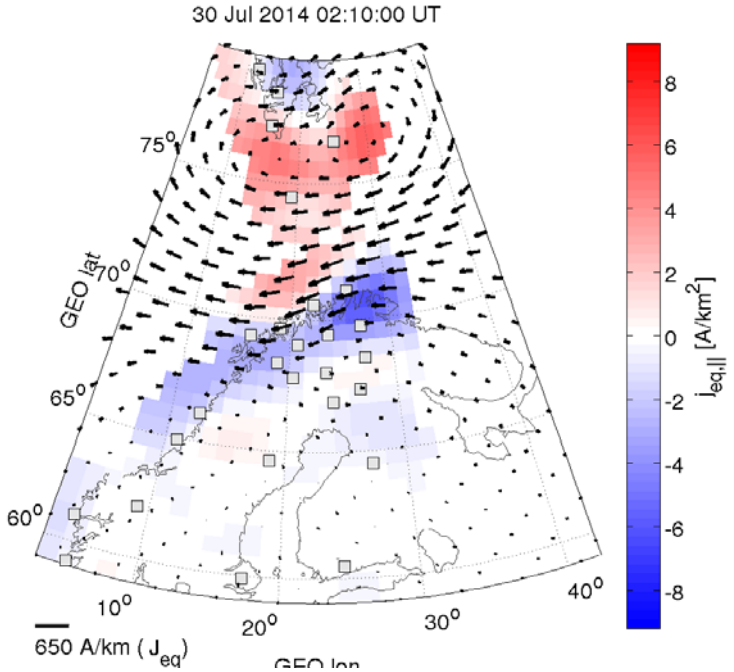

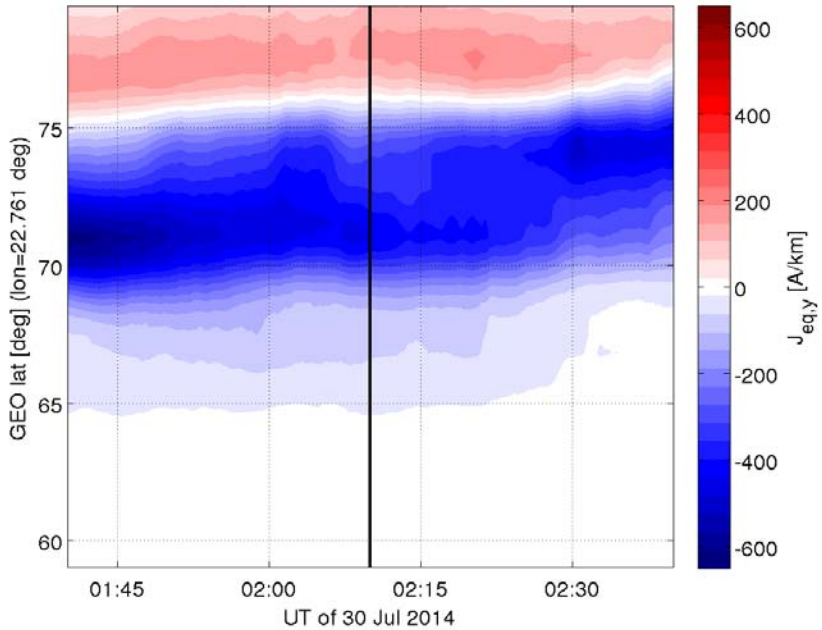

C. Input data: dB, E_OPER, E_PREL

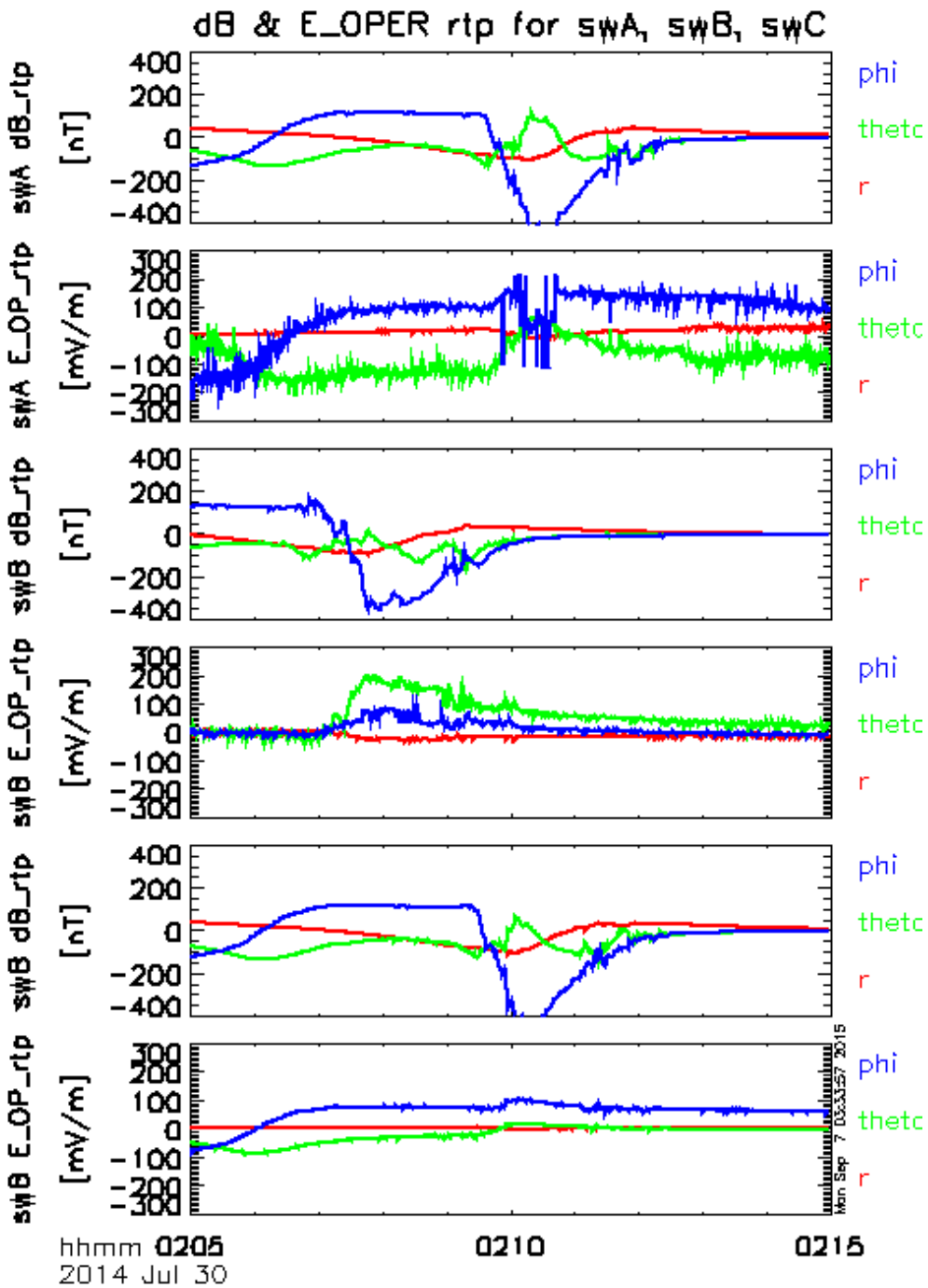

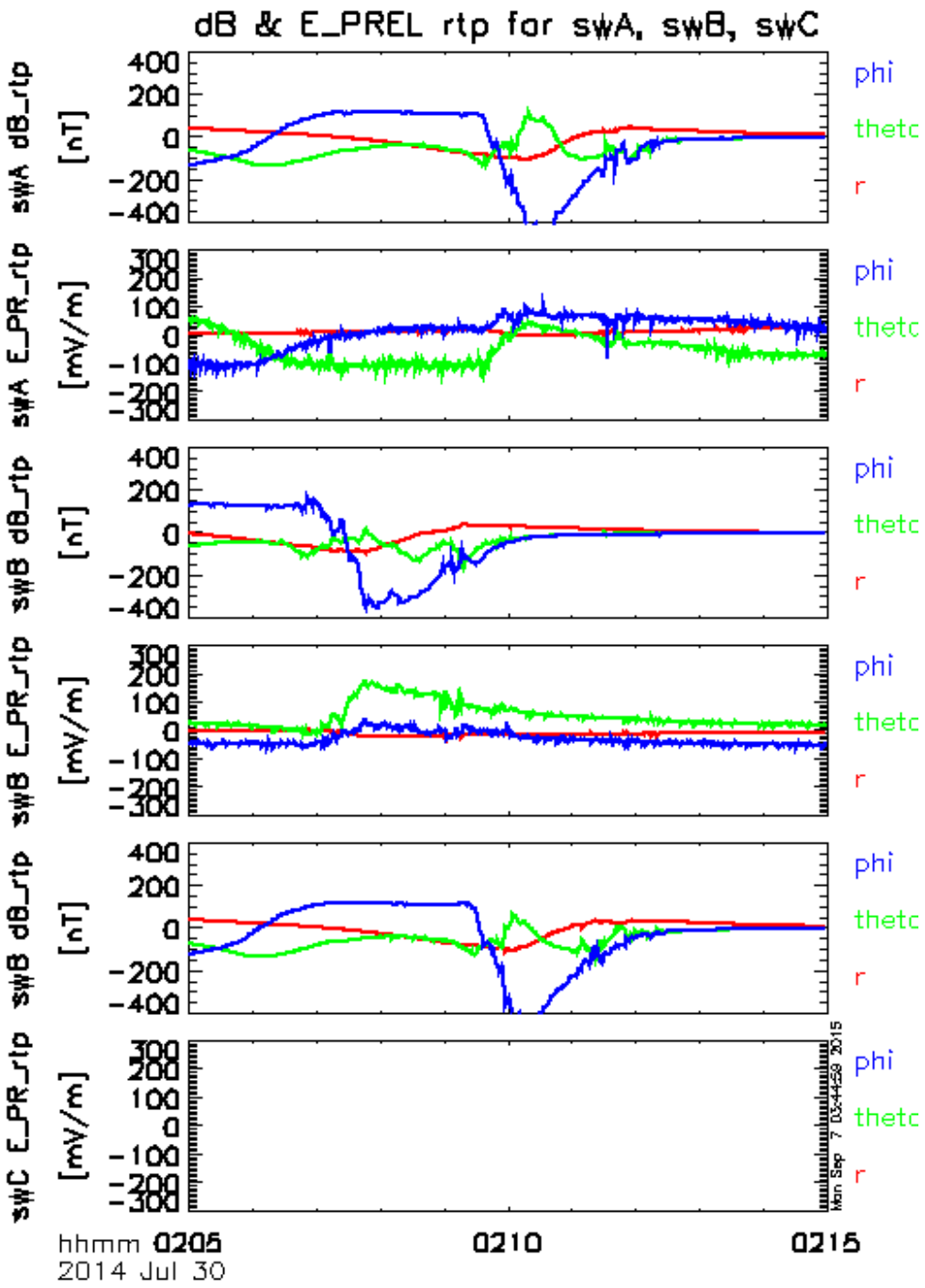

C. Grids

Narrow grid

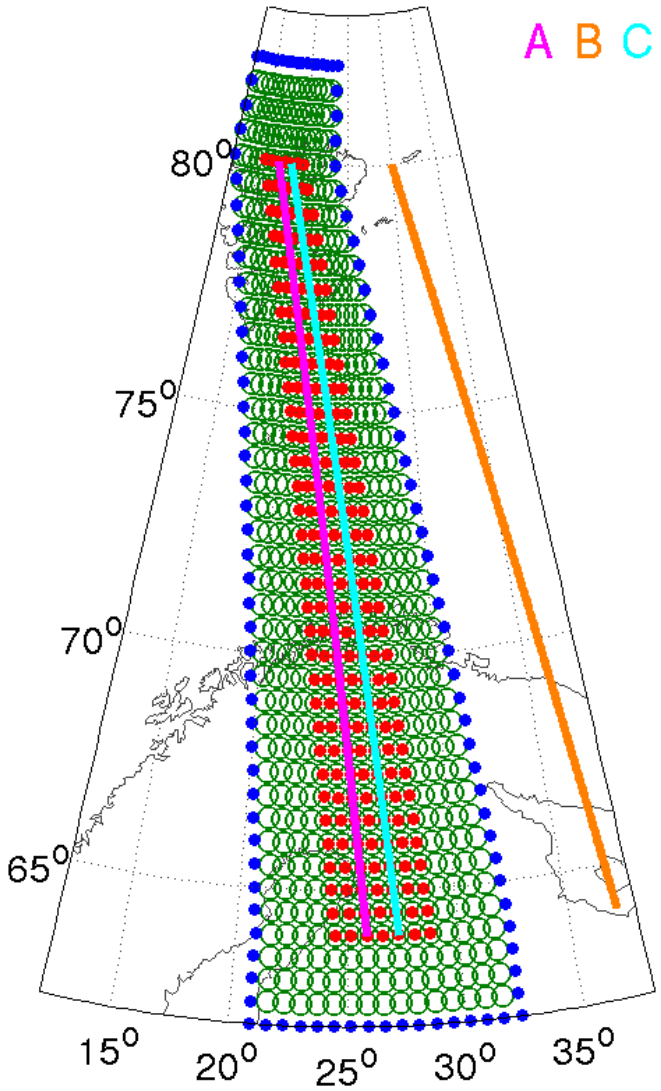

Large grid

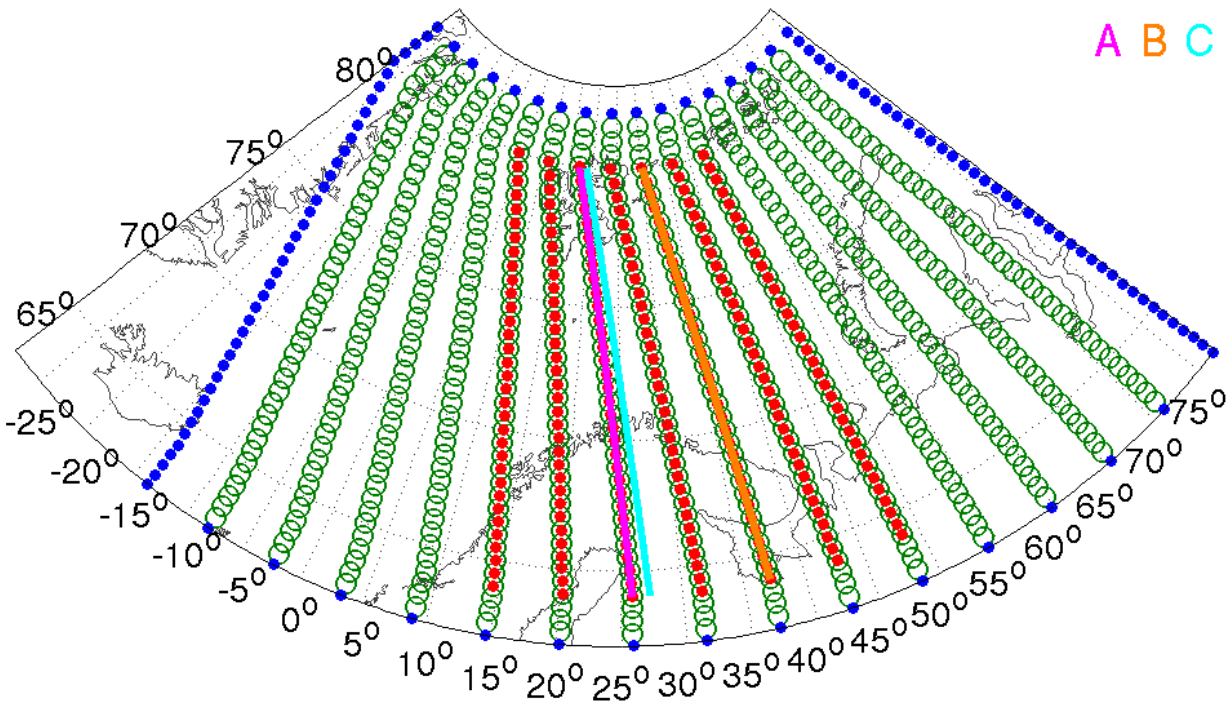

C. Results – OPER AB

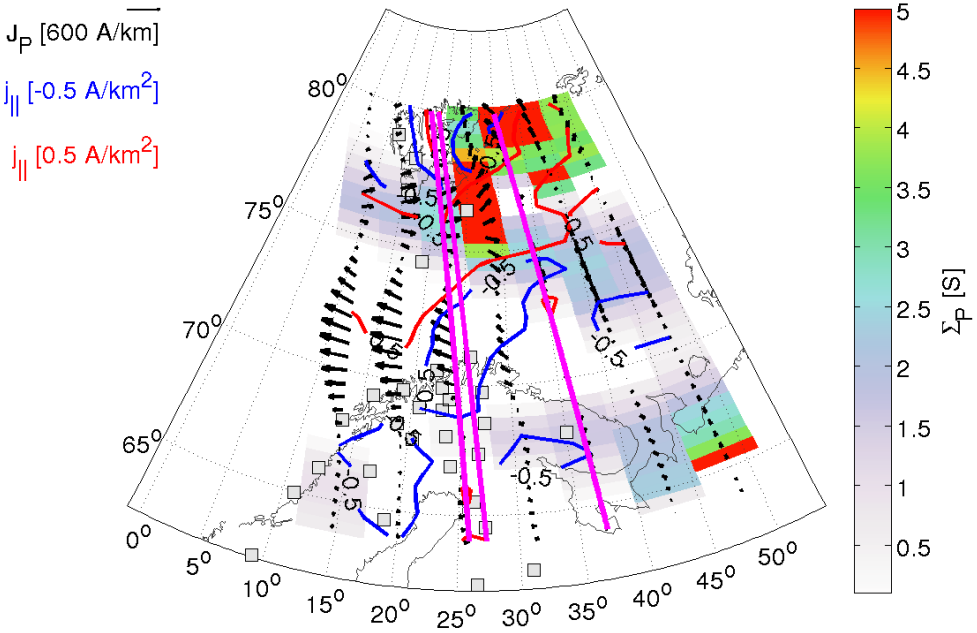

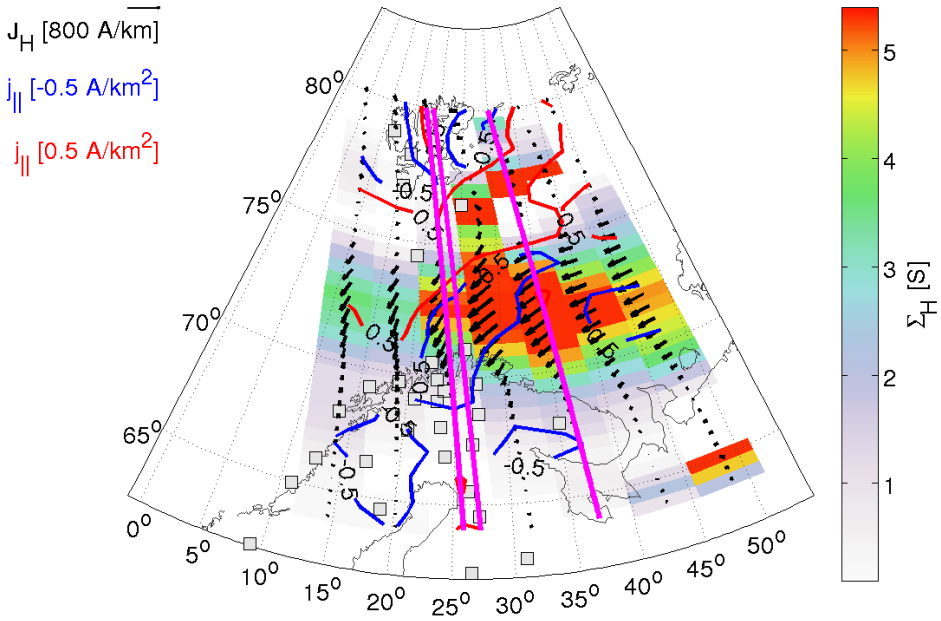

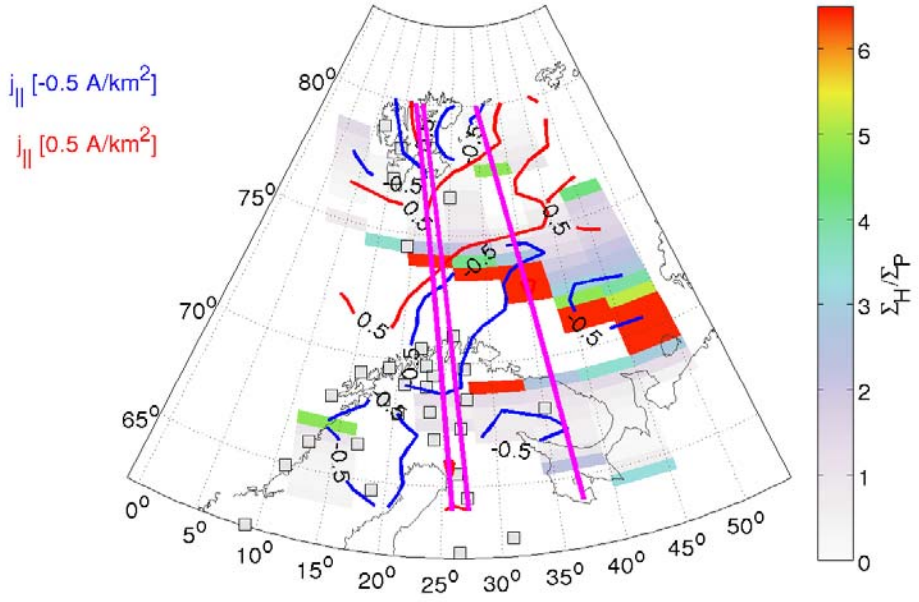

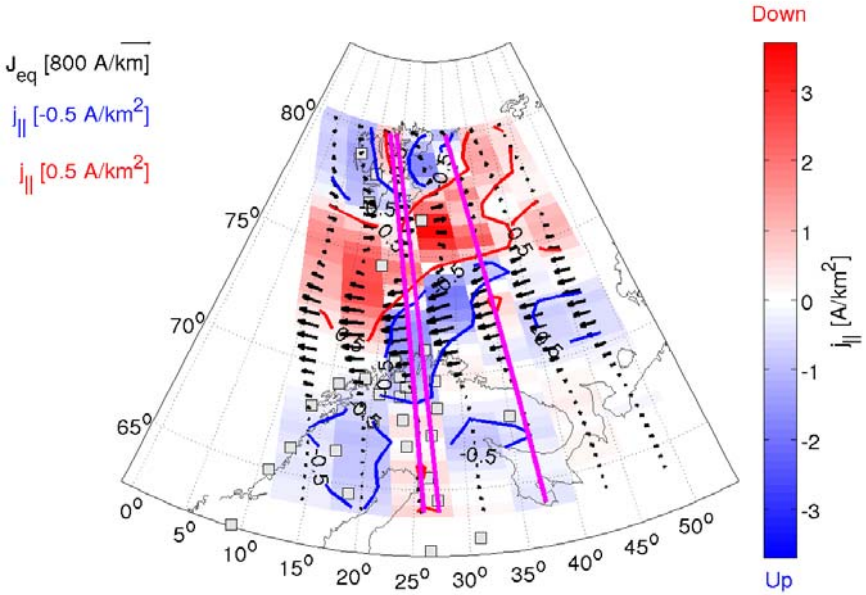

C. Results – OPER AB

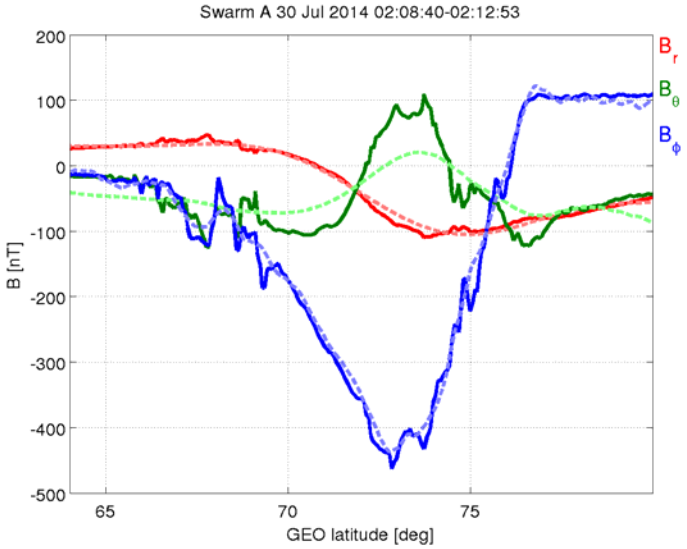

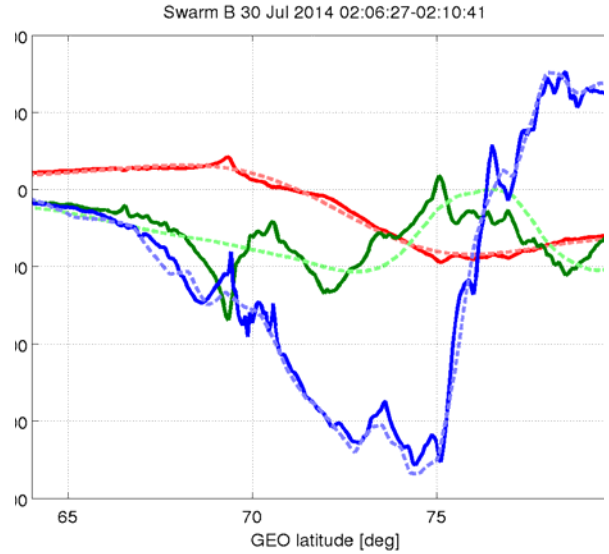

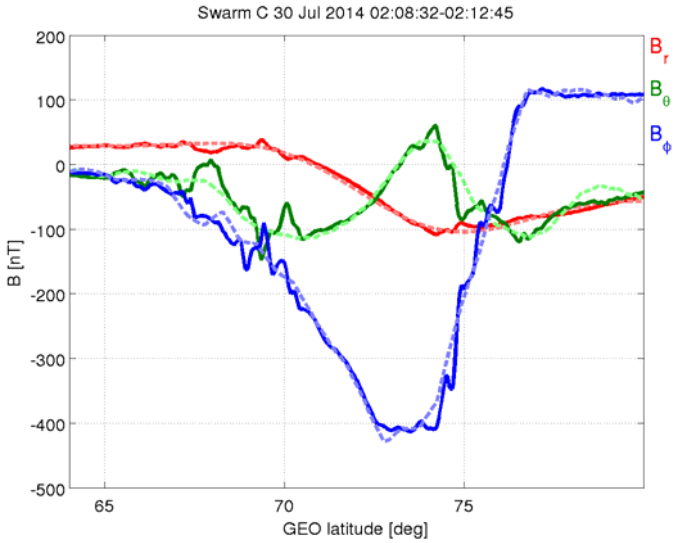

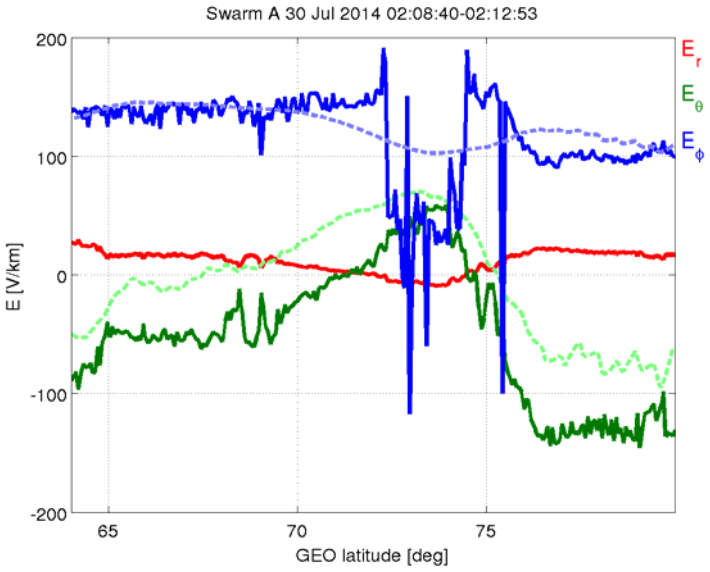

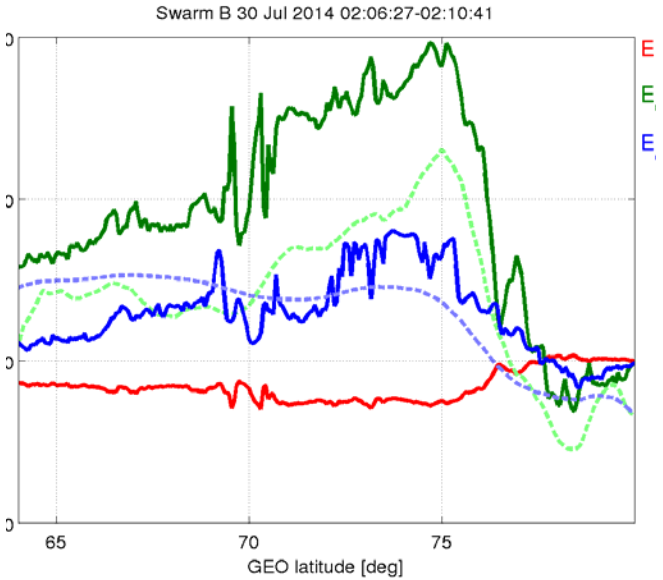

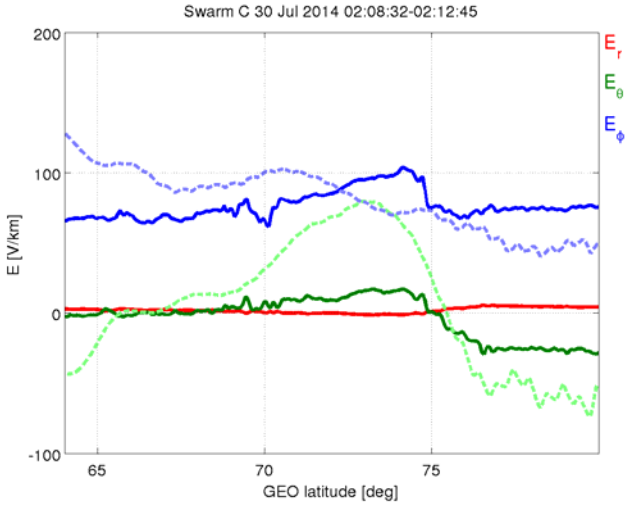

C. Results – OPER AB

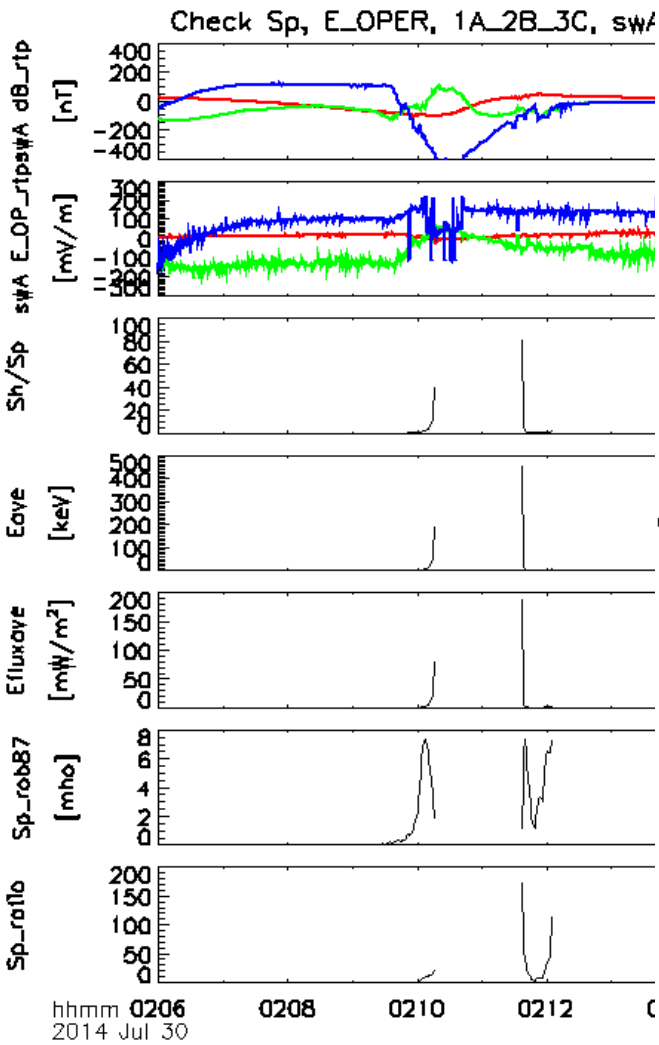

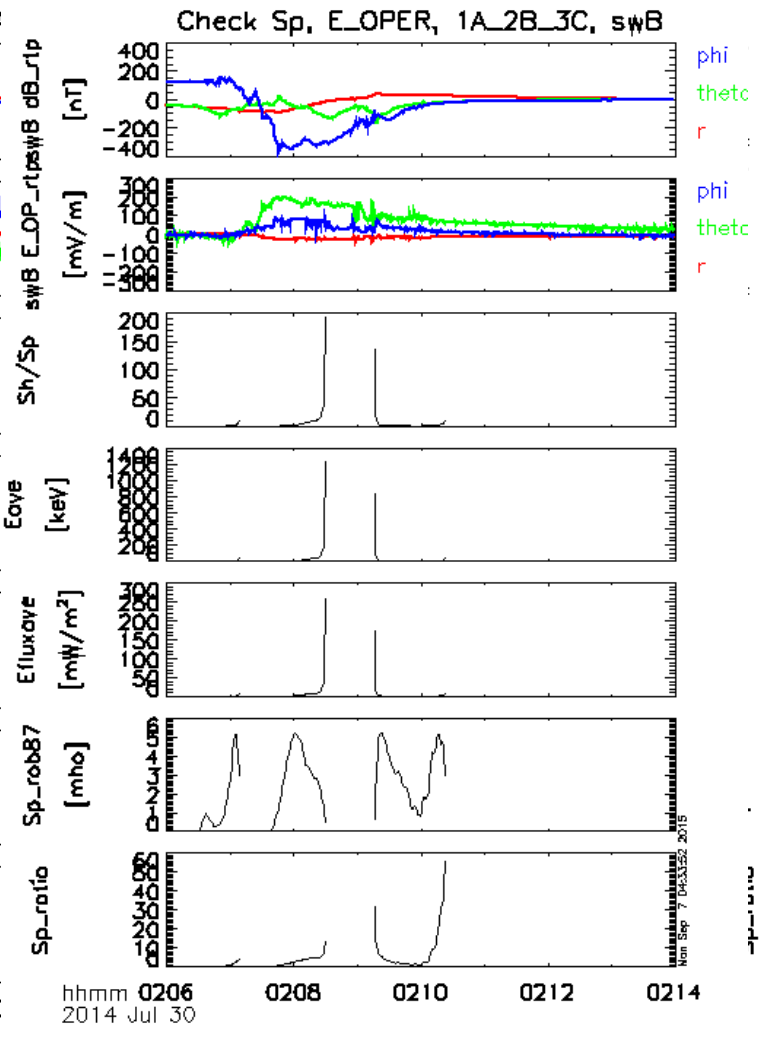

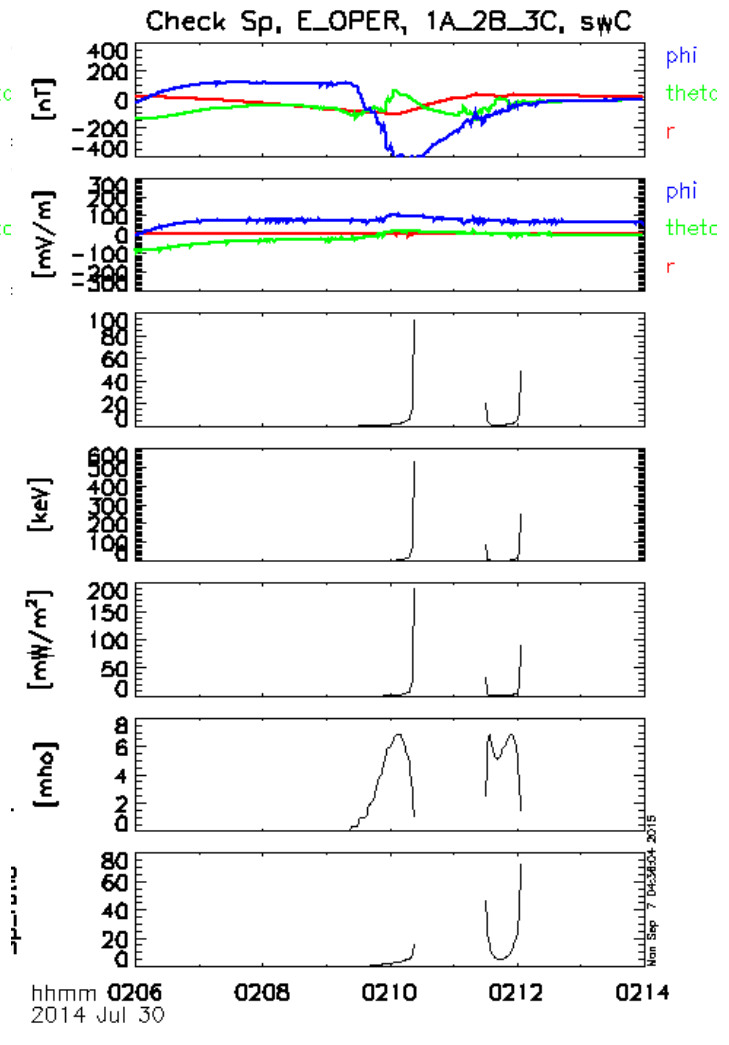

D. Polishing E

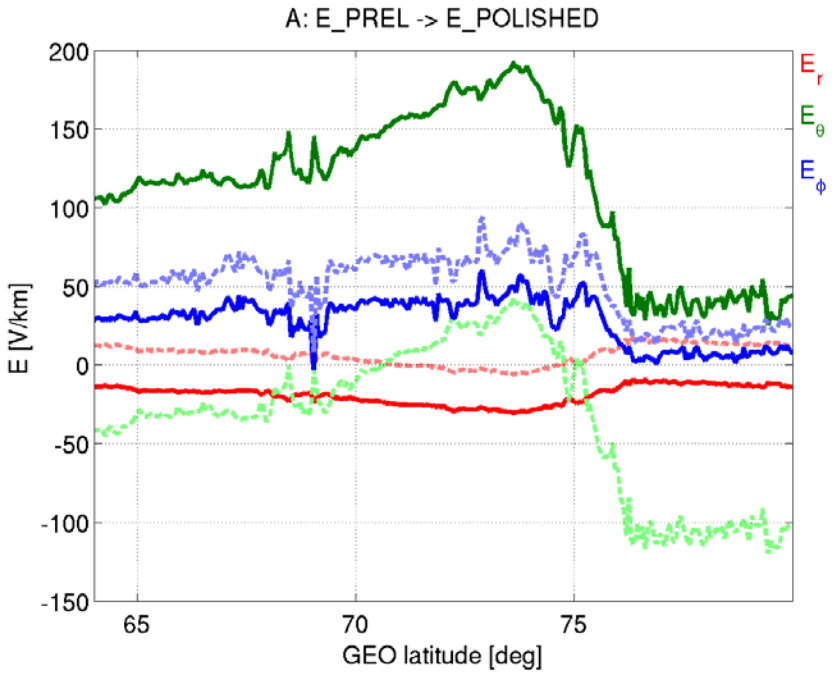

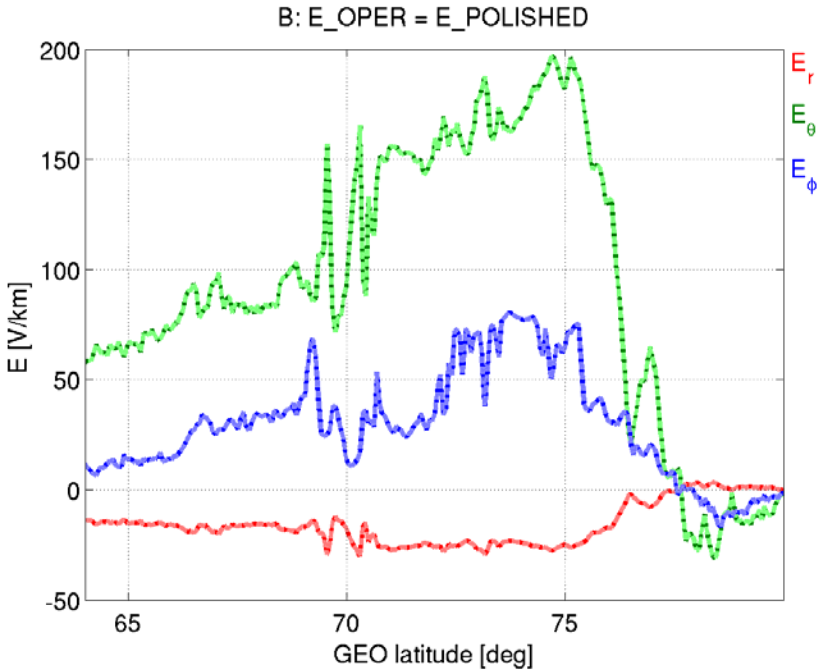

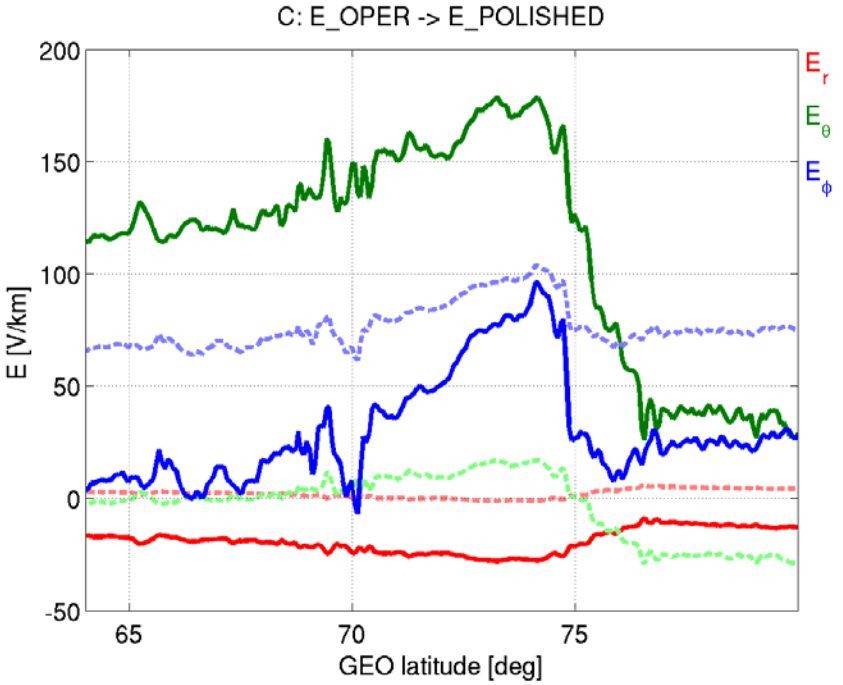

- **swA: E_PREL -> E_PREL_polished**
  - **Er_polished=-24.898+0.921*Er**
  - **Eθ_polished=148.768+1.029*Eθ**
  - **Eϕ_polished= -8.929+0.733*Eϕ**
- **swB: E_OPER**
- **swC: E_OPER -> E_OPER_polished**
  - **Er_polished=-24.764+2.724*Er**
  - **Eθ_polished=122.071+3.291*Eθ**
  - **Eϕ_polished=-155.986+2.427*Eϕ**

D. Results – E_polished AC

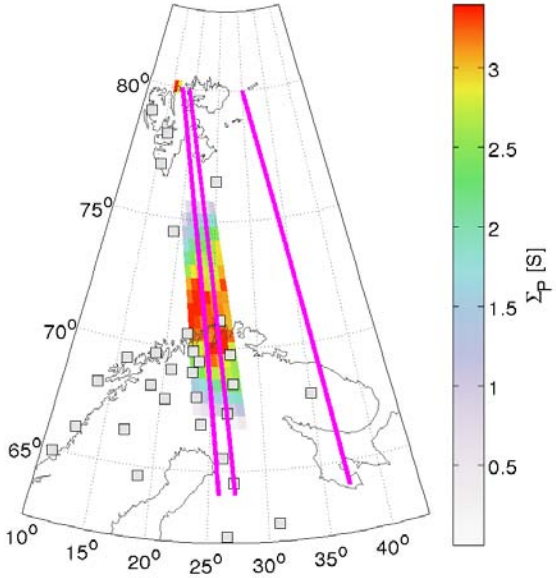

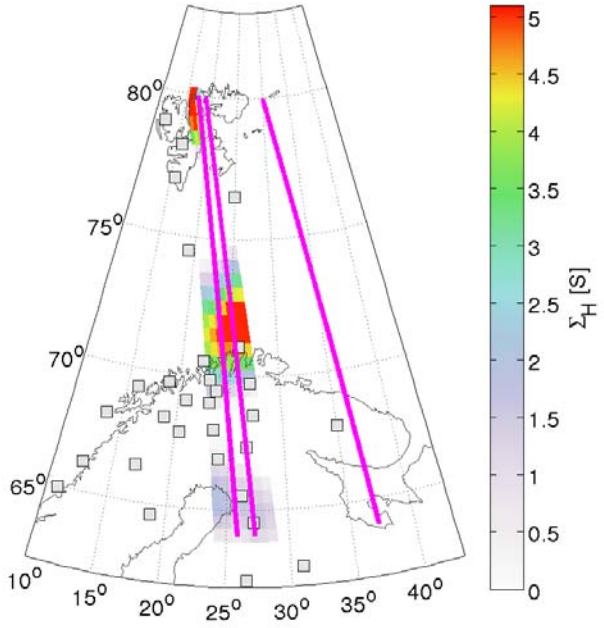

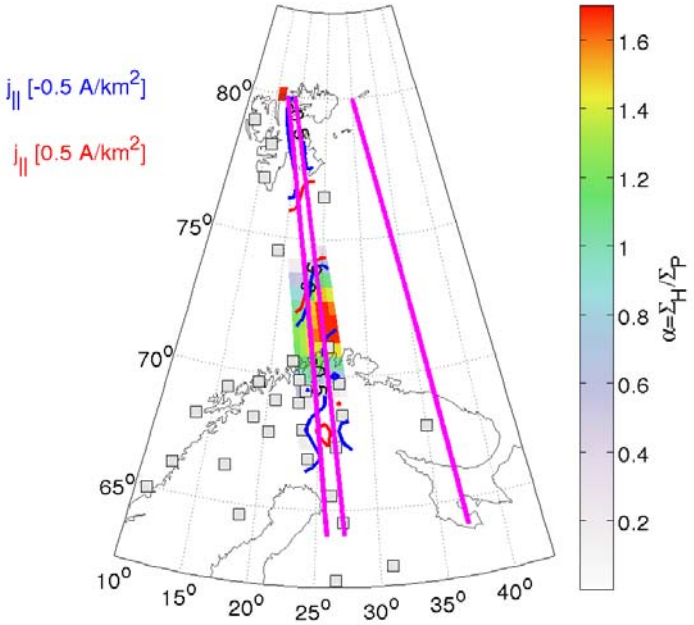

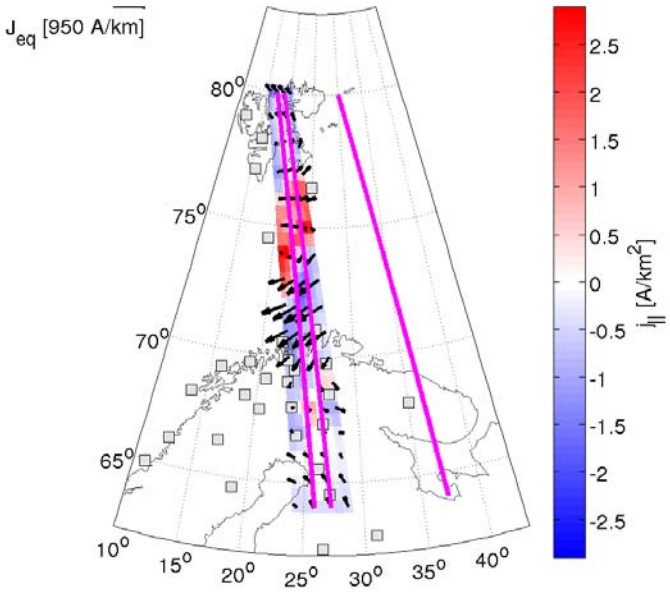

D. Results – E_polished AC

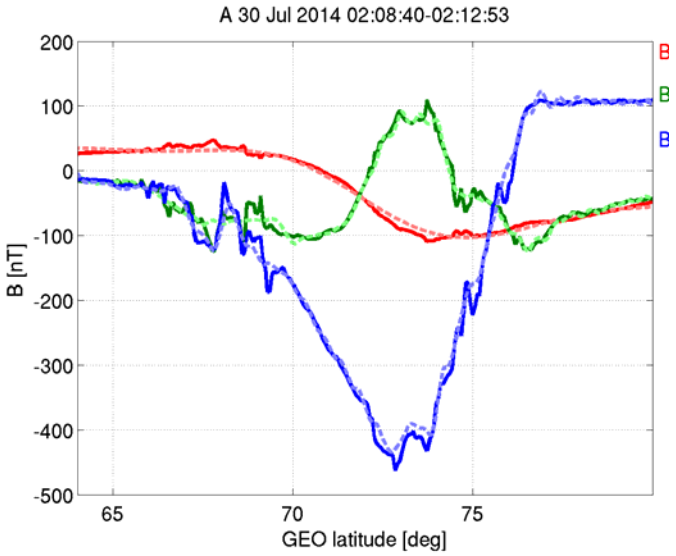

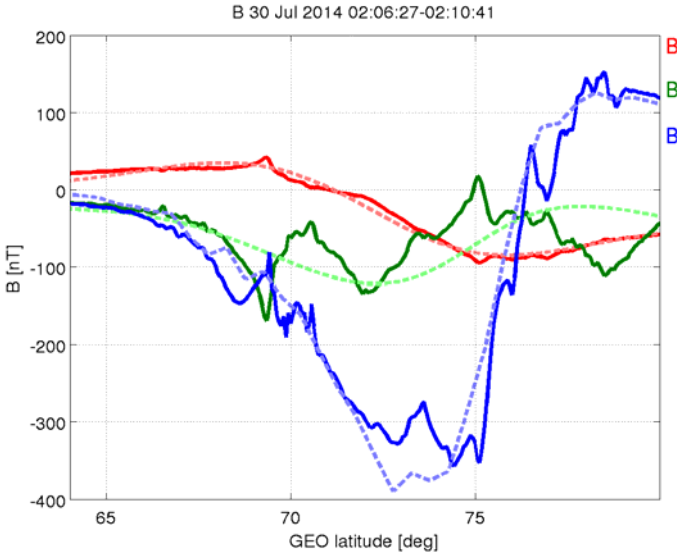

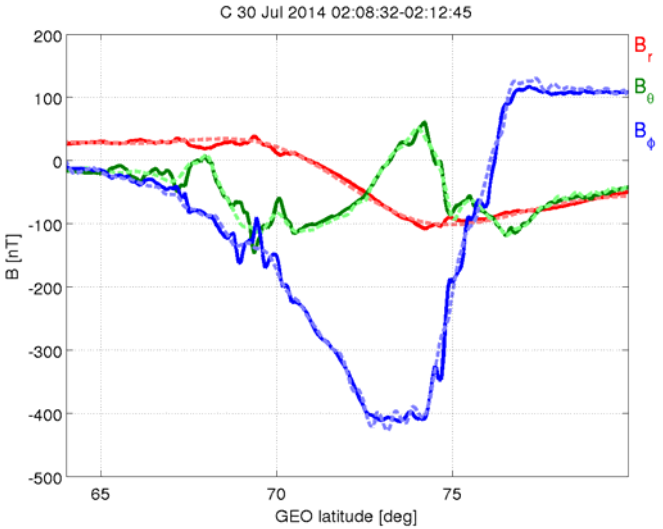

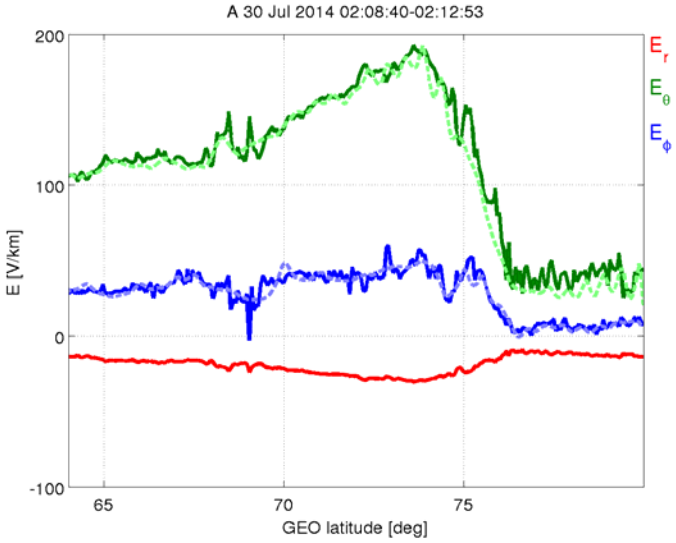

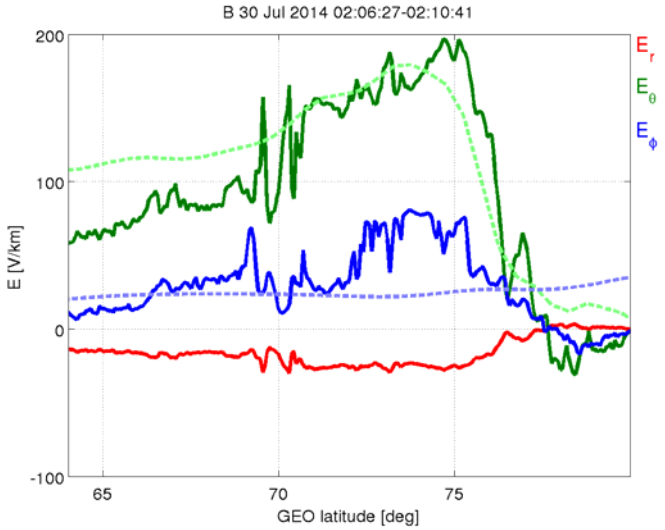

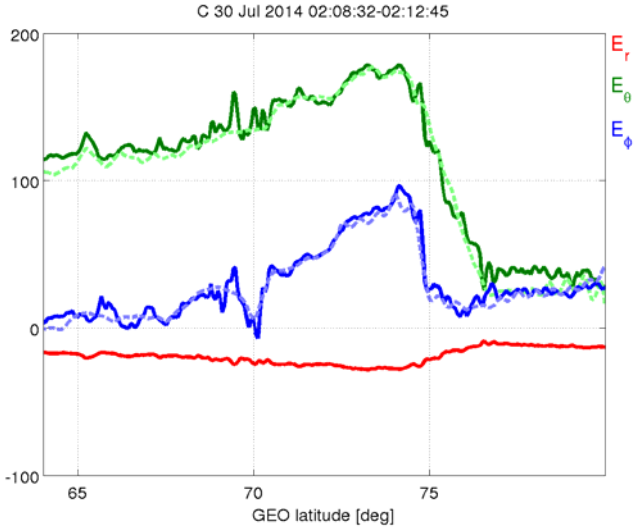

D. Results – E_polished AC

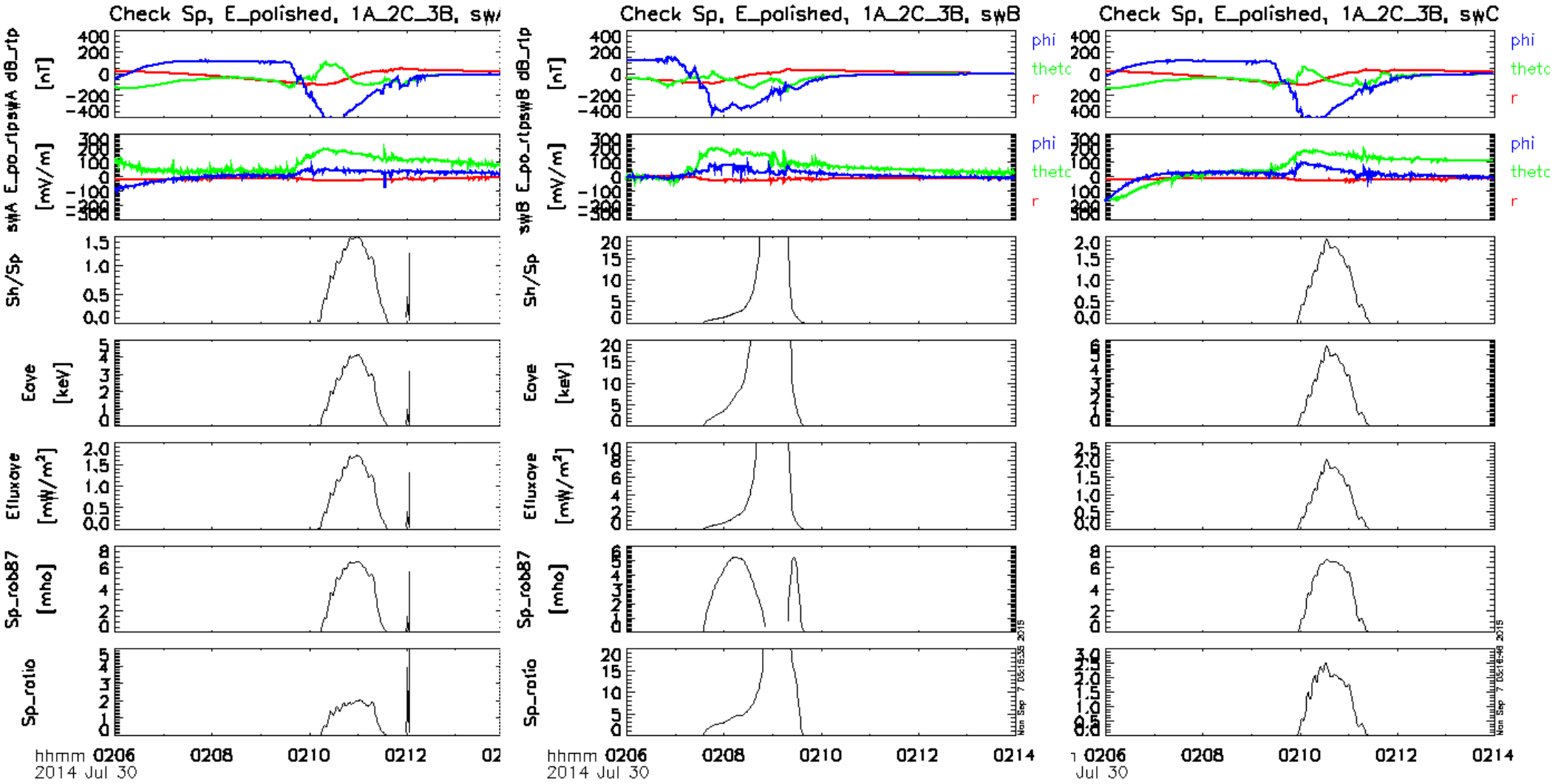

del

- α=ΣH/ ΣP, high in the regions where energetic precipitation and thus strong currents in the altitudese around 100 km
- Jϕ and Jθ derived from CHAMP data (2001-2002, 6112 overflights)
- Use the following formulas:

- Assumptions:
  - **B** radial, convection **E** horizontal
  - Eϕ <<E θ (not applicable in Harang discontinuity region)

$$\boldsymbol{J} = \Sigma_P \boldsymbol{E} - \Sigma_H \frac{\boldsymbol{E} \times \boldsymbol{B}}{B}$$

$$\boldsymbol{J} = \underbrace{(\Sigma_P E_\theta + \Sigma_H E_\phi)}_{=J_\theta} \hat{\boldsymbol{e}}_\theta + \underbrace{(\Sigma_P E_\phi - \Sigma_H E_\theta)}_{=J_\phi} \hat{\boldsymbol{e}}_\phi .$$

$$\alpha = \frac{\Sigma_H}{\Sigma_P} = \frac{\frac{E_\phi}{E_\theta} + \left(-\frac{J_\phi}{J_\theta}\right)}{1 - \left(-\frac{J_\phi}{J_\theta}\right) \cdot \frac{E_\phi}{E_\theta}}, \qquad \alpha = -\frac{J_\phi}{J_\theta}$$

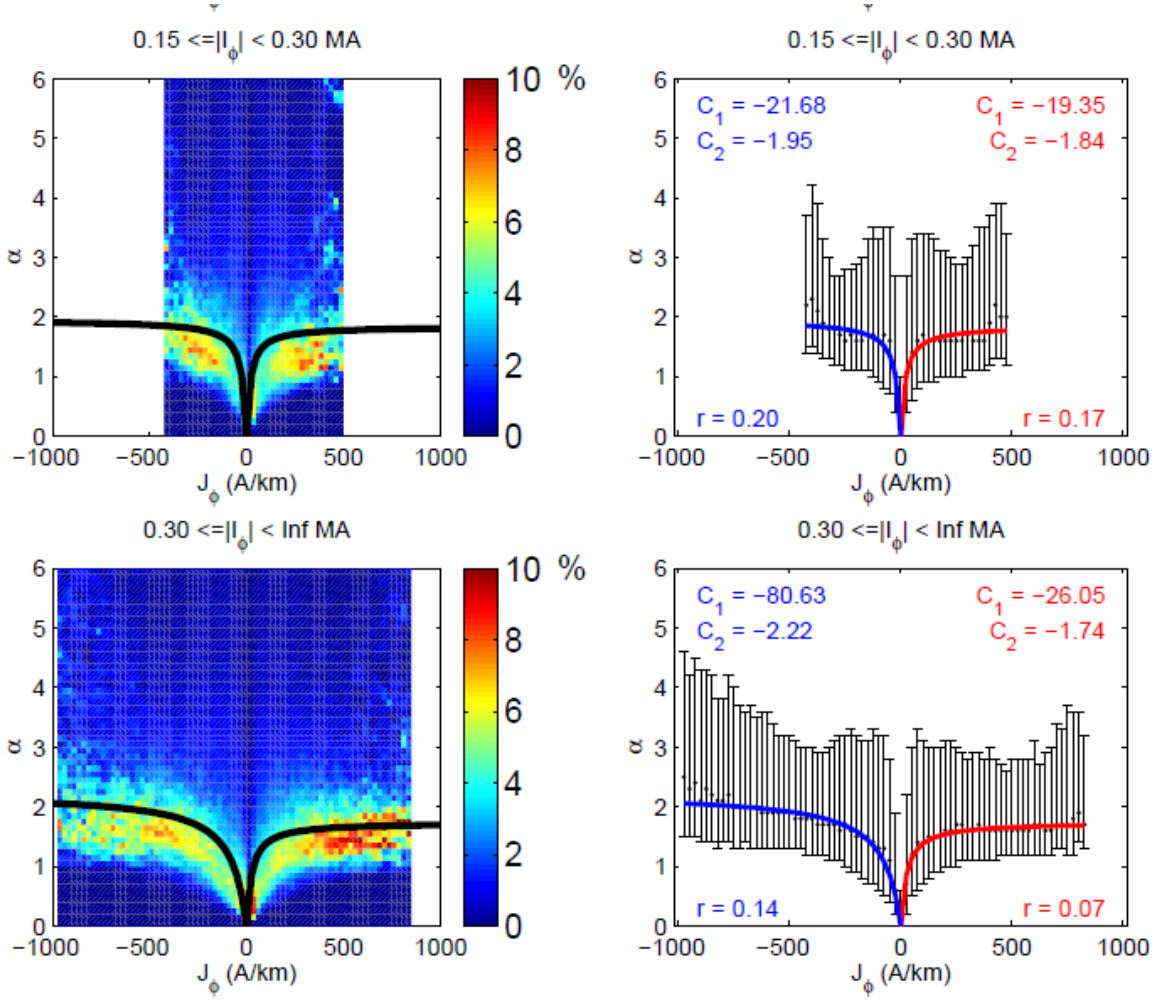

A statistical fit to Champ data which can be used also with GB magnetometers measuring Jφ

$$\alpha = -\frac{J_\phi}{J_\theta} = \frac{C_2}{\frac{C_1}{|J_\phi|} - 1}$$

Probability of different
α=Jφ/Jθ
as function of Jφ

Bin	C_1 (J_ϕ<0)	C_2 (J_ϕ<0)	C_1 (J_ϕ>0)	C_2 (J_ϕ>0)
All	−36.54	−2.07	−14.79	−1.73
Quiet	−20.35	−2.19	−46.16	−2.53
Moderate	−21.68	−1.95	−19.35	−1.84
Active	−80.63	−2.22	−26.05	−1.74
Winter	−21.87	−1.99	−13.79	−1.42
Equinox	−49.36	−2.10	−16.55	−1.63
Summer	−18.64	−1.86	−5.88	−1.76

Checking with α-parameter

SECS, B and E-field

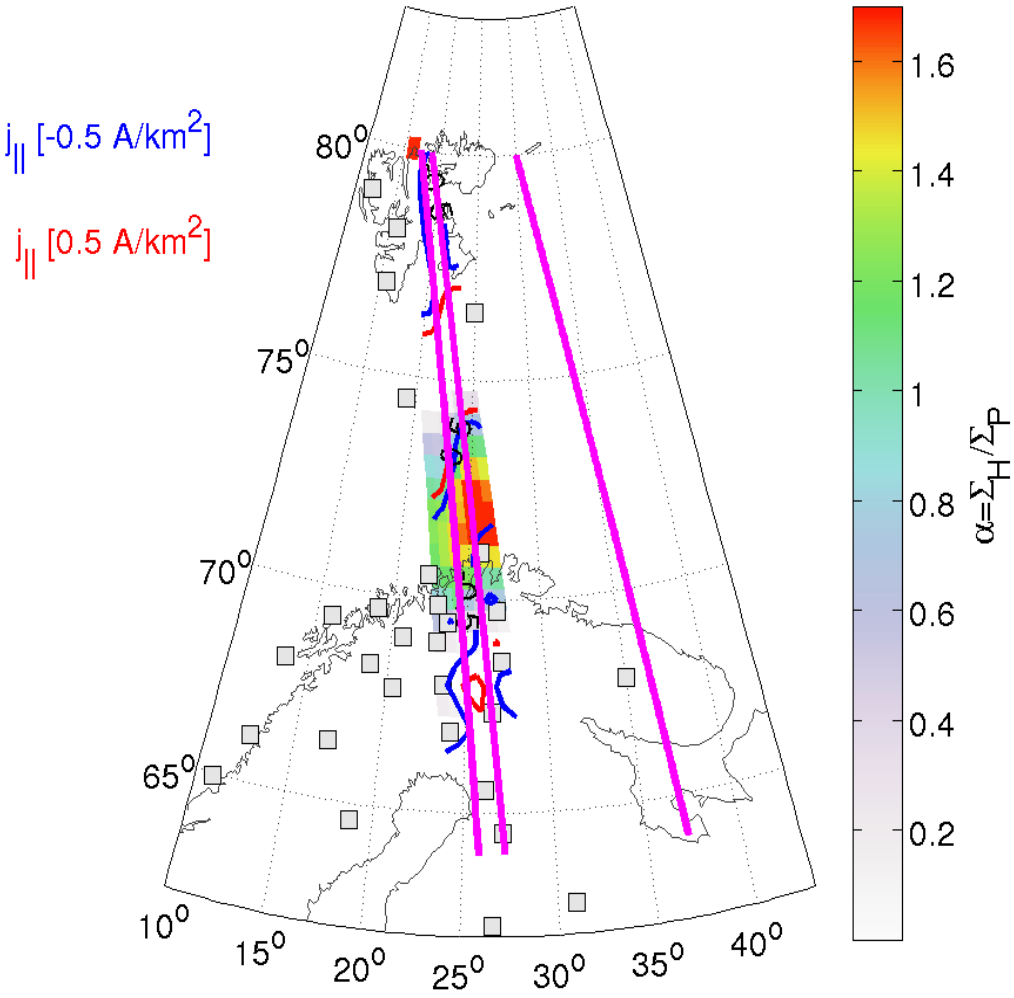

Champ statistics, only B field

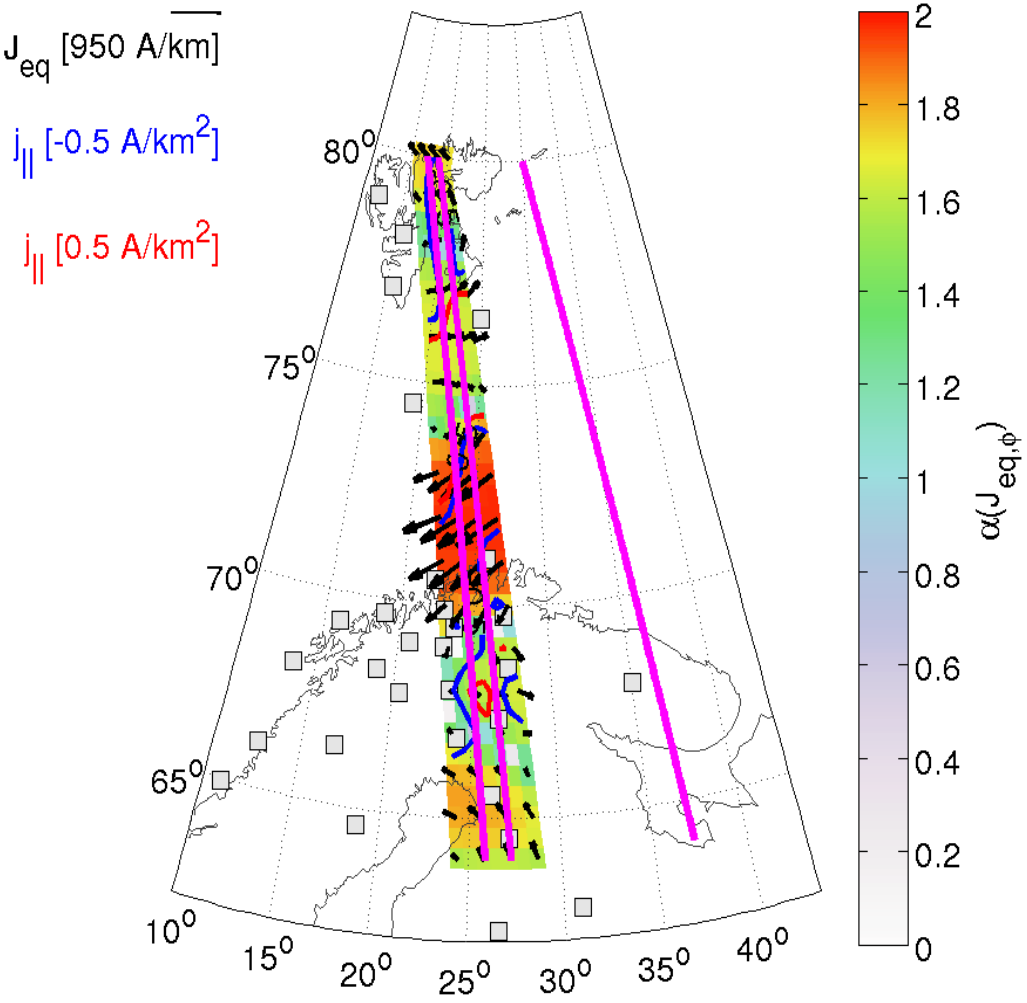

C. Auroral current circuit

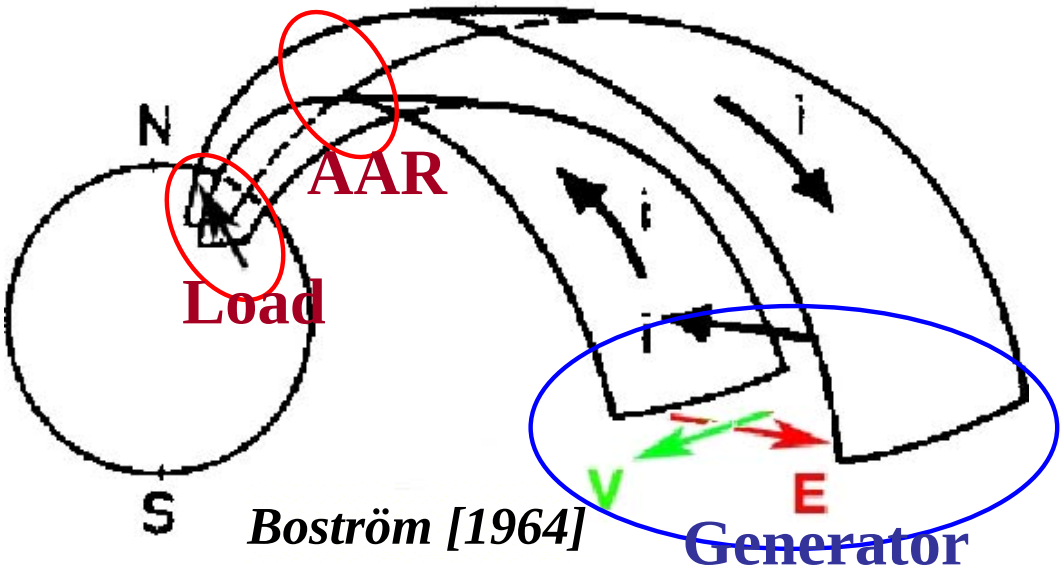

Boström [1964]

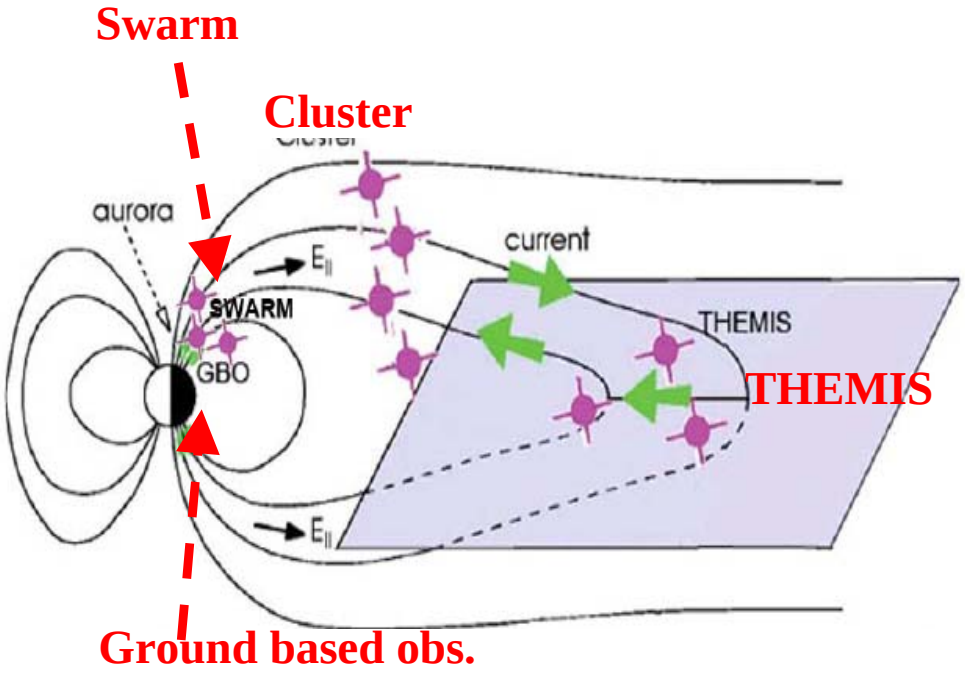

- **Comprehensive, multi-point exploration of the auroral current circuit, including:**
  - **the high altitude auroral generator in the magnetosphere, to be sampled by THEMIS, later also by MMS;**
  - **the auroral acceleration region at around 1 R_E, to be probed by Cluster;**
  - **the ionospheric load, to be observed by Swarm and ground observatories.**
- **While triple conjunctions will be rare (if at all), double conjunctions may occur more often, either with Cluster or with THEMIS / MMS.**